Early Holocene ritual complexity in South America: the archaeological record of Lapa do Santo (east-central Brazil)

André Strauss[1,2,3,4,*], Rodrigo de Oliveira[3,5], Ximena Villagran[6], Danilo Bernardo[7], Domingo Salazar-Garcia[2,8,9,10], Marcos César Bissaro Jr.[11], Francisco Pugliese[6], Tiago Hermenegildo[12], Rafael Santos[13], Alberto Barioni[3,14], Emiliano de Oliveira[3], João Carlos Moreno de Sousa[15], Klervia Jaouen[2], Max Ernani[3], Mark Hubbe[16], Mariana Inglez[3], Marina Gratão[3], H. Rockwell[17], Márcia Machado[18], Gustavo de Souza[19], Farid Chemale[20], Koji Kawashita[21], Tamsin O'Connell[12], Isabel Israde[22], James Feathers[23], Claudio de Castro[24], Michael Richards[2], Joachim Wahl[1,25], Renato Kipnis[3], Astolfo Araujo[6] & Walter Neves[3]

[1] *Senckenberg Centre for Human Evolution and Palaeoenvironment, Eberhard Karls Universität Tübingen, Geschwister-Scholl-Platz, 72074 Tübingen, Germany*

[2] *Department of Human Evolution, Max Planck Institute for Evolutionary Anthropology, Deutscher Platz 6, 04103 Leipzig, Germany*

[3] *Departamento de Genética e Biologia Evolutiva, Universidade de São Paulo, Rua do Matão 277, Cidade Universitária, São Paulo, SP, Brazil*

[4] *Centro de Arqueologia Annette Laming Emperaire, Av. Acdo. Nilo Figueiredo 2, Miguel A Salomão, Lagoa Santa, MG, Brazil*

[5] *Departamento de Prótese, Universidade de São Paulo, Av. Professor Lineu Prestes 2227, Cidade Universitária, São Paulo, SP, Brazil*

[6] *Museu de Arqueologia e Etnologia, Universidade de São Paulo, Av. Prof. Almeida Prado 1466, Butantã, São Paulo, SP, Brazil*

[7] *Instituto de Ciências Humanas e da Informação, Universidade Federal do Rio Grande, Av. Itália KM 8, Carreiros, Rio Grande, RS, Brazil*

[8] *Department of Archaeology, University of Cape Town, Private Bag X3, Rondebosch 7701, South Africa*

[9] *Archaeogenetics, Max Planck Institute for the Science of Human History, Kahlaische Strasse 10, 07745 Jena, Germany*

[10] *Departament de Prehistòria i Arqueologia, Universitat de Valencia, Avda. Blasco Ibáñez 28, 46010 Valencia, Spain*

[11] *Faculdade de Filosofia, Ciências e Letras de Ribeirão Preto, Universidade de São Paulo, Av. Bandeirantes 3900, Vila Monte Alegre, Ribeirão Preto, SP, Brazil*

[12] *Department of Archaeology and Anthropology, University of Cambridge, Downing Street, Cambridge CB2 3DZ, UK*

[13] *Fundação Nacional do Índio, Coordenação Regional Xavante, Barra do Garças, MT, Brazil*

[14] *Departamento de História e Geografia, Universidade de São Paulo, Av. Prof. Lineu Prestes 338, Butantã, São Paulo, SP, Brazil*

[15] *Museu Nacional, Universidade Federal do Rio de Janeiro, Quinta da Boa Vista, São Cristóvão, Rio de Janeiro, RJ, Brazil*

[16] *Department of Anthropology, The Ohio State University, 174 W. 18th Avenue, Columbus, OH 43210, USA*

[17] *Department of Anthropology, University of Wyoming, 1000 E. University Avenue, Laramie, WY 82071, USA*

[18] *Laboratório de Design e Seleção de Materiais, Universidade Federal do Rio Grande do Sul, Av. Osvaldo Aranha 99, Porto Alegre, RS, Brazil*

[19] *Instituto do Patrimônio Histórico e Arqueológico do Brasil, Superintendência de Minas Gerais, Belo Horizonte, MG, Brazil*

[20] *Instituto de Geociências, Universidade Federal de Minas Gerais, Av. Antônio Carlos 6.627, Pampulha, Belo Horizonte, MG, Brazil*

[21] *Instituto de Geociências, Universidade de Brasília, Darcy Ribeiro ICC, Ala Central, Brasília, Brazil*

[22] *Instituto de Investigaciones de Ciencias de la Tierra, Universidade Michoacana de San Nicolás de Hidalgo, Avenida Universidad 1471, Fraccionamiento Real Universidad, Morelia, Mexico*

[23] *Department of Anthropology, University of Washington, 4218 Memorial Way Northeast, Seattle, WA 98105, USA*

[24] *Instituto do Coração, Universidade de São Paulo, Av. Dr. Enéas de Carvalho Aguiar 44, Pinheiros, São Paulo, SP, Brazil*

[25] *Archäologie, Landesamt für Denkmalpflege, Berliner Strasse 12, 73728 Esslingen, Germany*

** Author for correspondence (Email: andre_strauss@eva.mpg.de)*

Early Archaic, human skeletal remains found in a burial context in Lapa do Santo in eastern Brazil are providing a rare glimpse into the lives of hunter-gatherer communities in South America, including their rituals for dealing with the dead. These included the reduction of the body by means of mutilation, defleshing, tooth removal, exposure to fire and possibly cannibalism, followed by the secondary burial of the remains according to strict rules. In a later period, pits were filled with disarticulated bones of a single individual without signs of body manipulation, demonstrating that the region was inhabited by dynamic groups in constant transformation over a period of centuries.

Keywords: Brazil, Lapa do Santo, early Archaic period, mortuary rituals

Supplementary material

1. Location and excavations methods

Lapa do Santo is located in Lagoa Santa region, eastern central Brazil (Figure 1). Lagoa Santa is an environmentally protected area comprising 360 km^2. The vegetation is dominated by savanna (*cerrado)* and semi-deciduous forest. The rivers Mocambo, Samambaia, Jaguara and Gordura make up a tributary net that flows west to east to Velhas River, the main river in the area. Geomorphologically Lagoa Santa is a karstic terrain that can be divided into four distinct domains: 1) below 660 meters above sea level (masl) the terrain is characterized by a fluvial plain connected with the regional base level (Velhas River); 2) between 660 and 750 masl there is a karstic plain with dolines and lakes 3) between 750 and 850 masl there are karstic plateaus characterized by the presence of limestone outcrops (reaching up to 75 meters in height); 4) above 850 masl residual peaks composed of the non-soluble metasedimentary rocks from the Serra da Santa Helena Formation.

The Lagoa Santa region geology comprises Sete Lagoas Formation and Serra da Santa Helena Formation, both part of the Upper Proterozoic metassediments of the Bambuí Group (Viana *et al.* 1998) of the São Francisco craton. This cratonic cover metamorphosed during the Brazilian Cycle (700-450 million years ago) in a process that resulted in planar structures, such as lineation and foliation, and sub-vertical structures, such as normal and revert faults. The combination of these structures provides the path for the geomorphologic evolution that leads to the rockshelter configurations found in the region. The regional rockshelters and outcrops are developed in the limestone of the Sete Lagoas Formation. More specifically, Lapa do Santo rockshelter developed in the Member Pedro Leopoldo that is composed by very pure limestones with more than 90% calcite (Viana *et al.* 1998).

The annual mean temperature is 23ºC, with lower temperatures (11ºC) occurring between June and July and higher temperatures (35ºC) occurring between October and November. The average humidity is around 65% in the dry season, from May to September, and around 85% on the rainy season, from November to April, with a pluviometrical mean of 1,400 mm/year. The major climatic characteristic of this region is the high concentration of rain during the rainy season (93% of total volume). When evaporation is analyzed, the region presents an annual deficit of 176 mm (Piló 1998). Despite these particular variations, the regional climate is classified as tropical, with a rainy summer and dry winter (Nunes *et al.* 2009). During dry periods, the above ground

water sources can become very scarce although underground drainages are capable of keeping the discharge in Velhas River.

The first human bones from Lagoa Santa were found by Peter Lund between 1835 and 1843 (Lund 1844; Cartelle 1994; Araujo *et al.* 2005; Piló & Auler 2002; Luna 2007). Due to the putative coexistence of man and megafauna Lagoa Santa became a well-known region for 19th-century scholars (e.g. Kollman 1884; Hansen 1888; Hrdlíčka 1912; Ten Kate 1885). During the 20th-century, different teams went to the region in order to find evidence that could confirm the coexistence hypothesis (Walter 1958; Walter *et al.* 1937; Hurt & Blasi 1969; Bányai 1997; Laming-Emperaire 1979). As a result of more than 170 years of excavations a large collection of early Holocene skeletons was formed. However, all those excavation were done in a time when proper documentation was not available and, therefore, they considerably lack contextual information. Coordinate by WAN and funded by São Paulo State Grant Foundation (FAPESP) the project "Origins and Microevolution of Man in America: a Paleoanthropological Approach" aimed to overcome this problem by identifying and excavating new sites in Lagoa Santa region.

Lapa do Santo was found in the frame of those efforts. Excavations took place between 2001 and 2009 under the coordination of RK, AGMA and DVB. Starting in 2001 several units were open in distinct areas of the shelter. It became apparent that the densest archaeological deposits were located in the south part of the shelter, immediately in front of the cave`s entrance. An ample excavation surface was established in this region becoming the Main Excavation Area (MEA, the pink area in Fig. 2). All human burials were found in the MEA. Excavations ended in 2009 when, according to Brazilian laws, the excavated area was filled with sediments recomposing the original topography of the shelter`s floor.

In 2011, a new excavation area was open in Lapa do Santo as part of another research project. Entitled "The Mortuary Rituals of the First Americans" and coordinated by AS this is a joint venture between the Department of Human Evolution of the Max Planck Institute for Evolutionary Anthropology (Germany) and the Laboratório de Estudos Evolutivos e Ecológicos Humanos da Universidade de São Paulo (Brazil). This new excavation is currently on-going and will not be discussed in the present contribution. The only exception to this concerns the undeformed samples for micromorphology. Since no undeformed samples were collected between 2001 and

2009 from the levels where the burials were found, the micromorphological analysis presented here is based on samples collected from the new excavation`s area at levels compatible with those from which the burials from LSMP-1, LSMP-2 and LSMP-3 come from. A detailed account on the formation processes studies on Lapa do Santo can be found in Villagran et al., (*in press*).

"Lapa" and "Santo" are the Portuguese words for, "rockshelter" and "saint". Lapa do Santo is a cave with an associated sheltered area of ca. 1300 m^2. The southern region of the sheltered area has a relatively flat, height and dry area located immediately in front of the cave's entrance. The floor of the shelter has a strong descending inclination towards the north, which becomes flat again near a natural sinkhole located at the northern extreme of the sheltered area (Figs. 2c-d).

A three-dimension coordinate system (x,y,z) was established in Lapa do Santo (Fig. 2a-b). The y-axis was conveniently oriented following the longer dimensions of the sheltered area, which is, in turn, roughly aligned with the geographic north-south axis (increasing towards the north). Therefore, the y-axis is also referred to as the north-south or N-S axis. The x-axis is perpendicular to the y-axis and is therefore roughly aligned with geographic east-west (increasing towards east). The x-axis is also referred to as the east-west or E-W axis. X-axis and y-axis define a horizontal plane. The z-axis is perpendicular to the plane defined by x-axis and y-axis and is therefore also referred to as the vertical axis or absolute depth (decreasing with progressive depth). The origin of the coordinate system (i.e. x=0, y=0, y=0) was conveniently positioned outside the sheltered area (see Figure 2). An aribitrary grid with squares of 1 meter per side was established starting from the origin of the coordinate system. In the x-axis, each one-meter interval was sequentially labeled with letters (A,B,C,D, etc.) and in the y-axis, each one-meter interval was sequentially labeled with numbers (1, 2, 3, 4, 5, etc.). The excavation of the site followed this grid and the unit's code refers to this system (e.g. L11, B13, Z14).

The excavations were based on natural depositional levels further divided into lithostratigraphic units (Gasche & Tunca 1983; Stein 1987; Stein 1992), which are composed of *facies*, to assure stratigraphic and spatial control of the archaeological remains (Stein 1987).

A f*acies* is the smallest stratigraphic/excavation unit, defined by its color, texture, hardness and inclusions. This concept of *facies* emphasizes the visible lithological changes that occur vertically and horizontally, representing any event over time resulting from the action of carriers bringing similarly sourced material and depositing them on the site (Stein & Rapp 1985). The depositional event that led to the formation of certain *facies* may have occurred on any time scale. The time of formation of the *facies* is not central to the definition of the term, only the fact that the same lithology was deposited continuously or sporadically brought no changes.

The lithostratigraphic unit hierarchically above the *facies* is defined by "*natural stratigraphic level*". This unit refers to the layer defined by the difference in color, texture and compositions observable in the field (bones, plants, rocks, etc.) representing qualitative differences along the strata excavation. A *natural level* may be composed of only one or more than one *facies*, with or without predominance between the *facies* (Stein & Rapp 1985). For each excavation unit, the *facies* were sequentially numbered (*facies* 1, *facies* 2, *facies* 3...).

The stratigraphic levels were also identified ordinarily with the surface level receiving the number 1. The change from one level to another was determined by changes in color, texture, hardness or composition of its constituent *facies*. However, in cases in which no changes occurred after excavating 10 cm, the level number was automatically changed. At the beginning of the excavation of each level, the z-value of the corners and the central portion of the correspondent unit was recorded. Within each level, their constituent *facies* were excavated separately. A sample of four liters of sediment was collected for flotation from each *facies* in each level. Flotation separated the material that sunk (heavy fraction) and that floated (light fraction). This material is currently under study.

All material of archaeological interest, i.e., lithic materials, bone, seeds, fruits, artifacts made of organic materials (wood, bone, plant) and charcoal, greater than 1 cm, were plotted using a total station according to the site's coordinate system. Each plotted piece received an identification number preceded by the prefix "St-". For each plotted piece, provenance information (unit, level and *facies*) was recorded. The material that could not be plotted (pieces smaller than 1cm found *in situ* or any piece recovered from the sieve) did not receive an identification number and can be tracked only based on its provenance information (unit, level and *facies*). The material was stored individually in

plastic bags with their identification cards. During the excavation all structured occurrences were excavated separately by stripping layers of archaeological material.

Archaeological excavation and documentation followed an Excavation Protocol created by one of the authors (RK) specifically for the project, so to ensure standardization of procedures within and between excavation teams. The excavations were documented independently for each unit using a Unit Excavation Form (UEF), Unit Schematic Drawing (USD), Unit Field Pictures (UFP), Worksheet of Spatial Registration (WSR), Worksheet of Volume of *Facies* (WVF), Notebooks of Excavation (NE) and Field Director's Diary (FDD).

Each level of each unit has a UEF. In this form the opening and closing z-values of the level were registered as well as the description of the excavated sediment (color, texture, hardness, inclusions). The USD is complementary to the UEF. Any noticeable feature or structure is registered in the USD (e.g., pebbles and/or boulder concentrations, fire hearths, sediment lens, roots, and animal holes). The USD is of particular importance since it is the most reliable tool to determine the spatial position of the burials in relation to the entire site.

Each unit has a WSR in which the x, y and z values of the plotted pieces are registered. In addition, the identification number and the provenance information were also recorded. This information is also available on the Identification Card that is kept together with the plotted piece. By duplicating the documentation, we minimized the risk of losing information. Each unit has a WVF in which the volume of each bucket of sediment is registered. This allows computing the exact volume of each excavated *facies* and levels. Each unit has an NE in which the excavator can note all his subjective impressions.

Concerning the exhumation of human burials, we adopted a method based on consecutive expositions. The exposition is the unit of the exhumation process. Each exposition must uncover the largest number of bones as possible, without implying the removal of any bone. When this stage is achieved no more sediment is removed and a detailed drawing (BSD) aided by the total station is made, each bone is individually identified, and photographic recording is done. After the BSD is done, the exposed bones are removed and the exhumation moves on, repeating the process until it is no longer possible to remove sediments without further removing bones. This is a very

meticulous process and sometimes a single burial might take as much as 20 days to be fully exhumed. The final result is a high-resolution documentation that allows a full reconstitution of the burial after its removal from the site.

In addition to the already mentioned sources of primary documentation, the burial exhumation processes also included the Burial Exhumation Form (BEF), Burial`s Schematic Drawing (BSD), Burial Field Pictures (BFP) and Laboratory Pictures.

The BEF is composed of two pages. In the first one information as the name of the responsible for the exhumation and the date of its occurrence is inserted. In addition, there are specific fields where information about the disposition of the skeleton should be added (flexed or extended, single or multiple, degree of articulation, angle of joints, etc.) The second page of the BEF has a schematic drawing of a skeleton used to indicate which bones were present. In addition, there is a field for the excavator to make a detailed description of the burial while it is being exhumed. The primary documentation was done in Portuguese and is available in digital format upon request.

2. Chronology

Lapa do Santo chronology is based on OSL dates from sediment, radiocarbon dates on charcoal and radiocarbon dates on human bone collagen. All samples were spatially controlled using a total station.

OSL

In total 21 sediment samples were collected for luminescence dating, including two outside the shelter in the lake basin (Table S1). The samples were mainly collected from test unit Q48 in the northern part of the shelter, from a T-shaped trench extending from the northern to southern part of the shelter, and from test units F13 and M6 in the south part of the shelter. Because this paper is focused on the burials coming from the main area of excavation, only the samples from F13 and M6 will be considered.

Samples were collected by driving light-tight cylinders into exposed profiles. After retrieval the ends were capped, and the samples shipped to Seattle. The caps were removed in subdued red/orange light. The end portions of the sample were used for dose rate measurements and the middle portion for luminescence measurements. Separate samples were collected to measure current moisture content.

Dose rate

Radioactivity was measured by alpha counting in conjunction with flame photometry for K. For alpha counting the pairs technique was employed to separate the U and Th decay series. Total K was measured on the flame photometer and converted to ^{40}K by natural atomic abundance. All samples were measured plus some additional strata or rocks that were near the samples and contributed to their dose rate. Radioactivity was also measured as a check by beta counting. Four assays were averaged and converted to beta dose rate (Bøtter-Jensen & Mejdahl 1988). This was compared with the beta dose rate calculated from the alpha counting and flame photometry results. $CaSO_4$:Dy dosimeters were placed at some of the sample locations but only a few were retrieved, because some of the excavation areas were not reopened. Dose rate information is given in Tables S2 and S3.

The beta dose rates, computed in the two ways mentioned, are compared in Table S3. A significant difference is only observed for UW1376, possibly because of some disequilibrium in the U decay chain. For this sample, the beta dose rate from beta counting, as a more direct measure, was used in age calculations. External dose rates from lab and dosimeter measurements are also compared in Table S3. For UW1376 there is a no significant difference. For UW1374, the difference is just barely significant at one-sigma. For UW1375, the difference was significant and the dosimeter was taken as the best measure of external dose rate. Current moisture content varied considerably throughout the shelter. For age calculation, the current content was used as the best estimate with a ± 5% error bar.

Although dose rates vary from different parts of the site, they are broadly similar within a single area. The samples from F13 have dose rates of about 1.8-2.3 Gy/ka, and the sample from M6 about 1.2 Gy/ka.

Equivalent dose

For luminescence measurements, the unexposed material from the samples is sieved, both wet and dry, to obtain appropriate size fractions. Both 150-180µm and 180-212µm fractions were used. These were treated with HCl and H_2O_2 to remove carbonates and organics. They were then etched for 40 minutes in 48% HF and rinsed with water, HCl and water again. Any grains remaining were passed through the 150µm or 180µm screen again to remove degraded feldspar. The material caught in the screen was density separated using a lithium metatungstate solution of 2.67 specific gravity to remove heavy minerals.

Grains were placed in specially-manufactured disks for single-grain measurement. Luminescence was measured on a Risø TL-DA-15 reader with single-grain attachment. Stimulation was by a 532nm laser delivering 45 W/cm^2. Detection of light was through 7.5 mm U340 (ultraviolet) filters. Exposure was for 0.8s on each grain at 125°C. The first 0.06s was used for analysis and the last 0.15s for background.

Equivalent dose (D_e), the laboratory estimate of total absorbed dose through time, was determined using the single-aliquot regenerative dose (SAR) protocol (Murray & Wintle 2000; Wintle & Murray 2006). The SAR method measures the natural signal and the signal from a series of regeneration doses on a single aliquot. The

method uses a small test dose (about 3 Gy in this case) to monitor and correct for sensitivity changes brought about by preheating, irradiation or light stimulation. SAR consists of the following steps: 1) preheat, 2) measurement of natural signal (OSL or IRSL), L(1), 3) test dose, 4) cut heat, 5) measurement of test dose signal, T(1), 6) regeneration dose, 7) preheat, 8) measurement of signal from regeneration, L(2), 9) test dose, 10) cut heat, 11) measurement of test dose signal, T(2), 12) repeat of steps 6 through 11 for various regeneration doses. A growth curve is constructed from the L(i)/T(i) ratios and the equivalent dose is found by interpolation of L(1)/T(1). A zero regeneration dose and a repeated regeneration dose are employed to insure the procedure is working properly. The preheat removes unstable signal. Both a 180°C and a 240°C preheat for 10 s were employed; no systematic differences in results were observed.

An advantage of single-grain dating is the opportunity to remove from analysis grains with unsuitable characteristics by establishing a set of criteria grains must meet. Grains were eliminated from analysis if they (1) had poor signals (as judged from errors on the test dose greater than 30 percent or from net natural signals not at least three times above the background standard deviation), (2) did not produce, within 20 percent, the same signal ratio (often called recycle ratio) from identical regeneration doses given at the beginning and end of the SAR sequence, suggesting inaccurate sensitivity correction, (3) yielded natural signals that did not intersect saturating growth curves, (4) had a signal larger than 10 percent of the natural signal after a zero dose, (5) produced a zero D_e (within 1-sigma of zero), or (6) contained feldspar contaminates (judged visually on growth curves by a reduced signal from infrared stimulation before the OSL measurement; done on two doses to lend confidence the reduction in signal is due to feldspar contamination). A dose recovery test was performed on some grains. The luminescence of the grains was first removed by exposure to the laser (using the same parameters mentioned earlier). A dose of known magnitude was then administered. The SAR procedure was then applied to see if the known dose could be obtained. Successful recovery is an indication that the procedures are appropriate.

D_e values were obtained on both 150-180μm and 180-212μm grains. The former sacrifices single-grain resolution because more than one grain will fit in the measuring holes, but comparison of D_e distributions between the two grain sizes yielded no differences that could not be accounted for by differential sample size. Using the

rejection criteria described earlier, an acceptance rate for all samples in the shelter of 10.9% was obtained for the 180-212μm fraction. It is 29.2% for the smaller size fraction, but the probability of both grains in the same hole having a usable signal is only 1.2%, and only 3.6% for one out of three. Averaging of signals from two or three grains is thus not expected to be significant, so the results from the two size fractions were pooled for further analysis. The most common reason for rejection was lack of measurable signal (91% of those rejected from the 180-212μm fraction). No other reason constituted more than 4% of the rejections.

The SAR protocol is designed for the fast component in quartz. Quartz is known to contain multiple traps that bleach at different rates. The fast component is the only stable one that bleaches rapidly. If grains are dominated by slower bleaching components, the SAR protocol may not yield the correct D_e value. One way to visualize component structure is to utilize linear modulated OSL (LM-OSL). Most OSL is measured in what is called continuous wavelength mode, where the power and the wavelength of the stimulating source are kept constant. In LM-OSL, the wavelength is kept constant, but the stimulating power is ramped from zero to full power. Electrons from rapidly bleaching peaks are preferentially released early, when power is still low, while electrons from slower bleaching peaks are released later. This provides a peak structure where the components can be visually distinguished.

LM-OSL was measured for several samples, including four under consideration here, at the end of an SAR sequence, following a dose approximately the size of the equivalent dose. The laser power was ramped from 0 to 90% power in 30s. A comparison was made among grains of the intensity ratio of the curve at 16% power and that at about 5.5% power. Those values were chosen as the point of the fast component peak (5.5%) and the point where the fast component drops to background (16%), as concluded from grains where the signal dropped the quickest. Grains with a ratio less than 0.2 were compared with those with a ratio greater than 0.6, the former taken as grains dominated by the fast component and the latter taken as grains with a significant medium or slow component. For all samples, grains with ratios less than 0.2 are much more common than those with ratios more than 0.6. Comparing the central age D_e values for each group shows either no significant difference or a smaller D_e for the higher ratio, which is the opposite one would expect if the slower components had much effect. Quartz in these samples appears then to be dominated by the fast component, and

in those few grains where slower components are present, the D_e values did not differ significantly from those dominated by the fast component.

Dose recovery was performed on 12 samples from the entire shelter with a total number of accepted measurements at 399. The central tendency (as measured by the central age model, discussed later) of the normalized results (obtained dose/given dose) is 1.03±0.01 with an over-dispersion of 13.5±1.4%. This suggests the procedures are satisfactory. Over-dispersion in dose recovery reflects only intrinsic causes (machine error, variation in luminescence properties of grains, etc.). All external causes, differential dose rate or differential age, are controlled. This means that for a single-aged sample, an over-dispersion of at least 15% should be expected. This is within the range reported for single-aged samples from many areas.

A D_e value is obtained for each suitable grain. Because of varying precision from grain to grain, the same value is not obtained for each grain even if all are of the same age. Instead a distribution is produced. The common age model and central age model of Galbraith (Galbraith & Roberts 2012) are statistical tools used in evaluation of D_e distributions. These models are used in reference to D_e and not "age" per se, although dividing the D_e values by the bulk dose rate provides an "age" for each grain (not accounting for differential dose rates for individual grains). The common age model controls for differential precision by computing a weighted average using log D_e values. The central age model is similar except rather than assuming a single true value it assumes a natural distribution of D_e values, even for single-aged samples, because of non-statistical sources of variation. It computes an over-dispersion parameter (σ_b) or that deviation beyond what can be accounted for by measurement error. For samples of mixed ages a finite mixture model is employed for evaluation (Galbraith & Roberts 2012). This uses maximum likelihood to separate the grains into single-aged components based on the input of a given σ_b value and the assumption of a log normal distribution of each component. The model estimates the number of components, the weighted average of each component, and the proportion of grains assigned to each component. The model provides two statistics for estimating the most likely number of components, maximum log likelihood (llik) and Bayes Information Criterion (BIC).

Table S4 gives the equivalent dose central age value and over-dispersion for each sample. Over-dispersion is higher than 15% for all samples, although not by much

for some. This suggests, overall, that some of the scatter in the distributions of D_e values has extrinsic causes.

To look at the structure of these distributions, a finite mixture model was applied, using 15% as the assumed minimum over-dispersion for a single-aged sample. The number of components detected and the percentage of the most common component are given in Table S4. Two samples, UW861 and UW1375 are consistent with a single age. The other samples appear more mixed.

One extrinsic cause of over-dispersion is differential dose rate, mainly affecting the beta dose rate because of heterogeneous distribution of either uncommon K-feldspars (the K from which can contribute a large part of the beta dose rate) or carbonate materials (such as speleothems) which contain little radioactivity. Grains close to K-feldspars or speleothem fragments will experience a different dose rate than grains further away. While no measurements of spatial distribution of radionuclides has been done, it is possible to model the possible effect to see if it could cause the observed D_e distributions. The effect of heterogeneous distribution of K was modeled following Mayya et al. (2006) using the procedure of delineated by David et al. (2007), while the effect of speleothems was modeled by just assuming that grains next to speleothem fragments would experience half the dose rate of other grains. In both cases, the ages of lower components are increased by assuming a minimum dose rate as determined from the models and comparing them with adjusted ages of higher components. Comparisons were between the two most common components. The difference between assuming K hotspots (i.e., areas of high radioactivity) or speleothem cold spots (low radioactivity) was not substantial, so either has about the same effect. The results show that these models can explain the difference in D_e for the two most common components for all of these samples. This is not to say that the models are an accurate description of the dose rate distribution. It is to say that beta dose rate heterogeneity cannot be ruled out for explaining the over-dispersion.

Given that beta heterogeneity can explain the over-dispersion and no obvious agent for large scale mixing presents itself, the central age model appears to represent the best estimator for determining equivalent dose. If beta heterogeneity is present, the central age model allows for averaging out the effects. It could also take into account small scale mixing, where there was movement both up and down, which might occur with trampling, for example.

Ages

Age is determined by dividing the central age equivalent dose by the bulk dose rate. Table S5 gives the ages for each sample. Single-, or near single-aged samples are italicized. As can be seen in Figure 3 samples UW861 and UW1377 are in complete stratigraphic agreement with the dated charcoals (see next section). The other three samples, however, are consistently older than charcoals found in equivalent depth (ie. z-values). No good explanation is available for that. According to the OSL samples the earliest human occupation appears to date from about 9.0 to 12.0 kyBP, consistent with other paleoindian occupations in Lagoa Santa. In the unit F13 dates from UW1374 and UW1375 are at least two thousand years older than the dates obtained from radiocarbon. In addition, there is a general lack of agreement between the vertical position of the OSL sample and the radiocarbon dates (see below). Therefore, we consider the OSL dates as generally supporting the early Holocene chronology of the oldest deposits but they cannot be relied on for more refined estimation of age of different strata.

Radiocarbon

At Lapa do Santo a total of 53 charcoal samples were selected for radiocarbon dating. The samples were sent to the Beta Analytic AMS system in Miami where they have been pretreated with the ABA method.

Fifty-eight human bone and teeth sampled from Lapa do Santo's burials were also sent to Beta Analytic between 2001 and 2009 and pretreated without ultrafiltration method. Nine samples provided collagen and carbon for accurate measurement. The measured ages were then corrected according to the $^{13}C/^{12}C$ sample ratio, from which the conventional age was derived.

Twenty-one fragments of human bone from Lapa do Santo were pretreated at the Department of Human Evolution, Max Planck Institute for Evolutionary Anthropology (MPI-EVA), Leipzig, Germany, using the method described by Talamo and Richards (Talamo & Richards 2011). The outer surface of the bone samples are first cleaned by a shot blaster and then 500mg of bone powder is taken. The samples are then decalcified in 0.5M aq. HCl at room temperature until no CO_2 effervescence is observed, usually

for about 4 hours. 0.1M aq. NaOH is added for 30 minutes to remove humics. The NaOH step is followed by a final 0.5M HCl step for 15 minutes. The resulting solid is gelatinized in a pH3 solution in a heater block at 75°C for 20h, following Longin et al., (Longin 1971). The gelatin is then filtered in an Ezee-Filter™ (Elkay Laboratory Products (UK) Ltd.) to remove small (<8 □m) particles. The gelatin is then ultrafiltered with Sartorius "Vivaspin 15" 30 KDa ultrafilters (Brown *et al.* 1988). Prior to using the filter is cleaned to remove carbon-containing humectants (Higham *et al.* 2006). The samples are then lyophilized for 48 hours.

C:N ratios, %C, %N, δ13C and δ15N values were measured at Max Planck using a Thermo Finnigan Flash EA coupled to a Delta V isotope ratio mass spectrometer. For acceptable quality collagen, the atomic C:N ratio should be between 2.9 and 3.4 and a collagen yield of more than 1% of weight (Ambrose 1990; van Klinken 1999; DeNiro 1985). For Lapa do Santo alI the isotopic results, C:N ratios and collagen yields are well within the accepted ranges (Table S6, attached as Excel File). Three out of 21 samples obtained enough collagen for radiocarbon dating and were sent to the Klaus-Tschira-AMS facility of the Curt-Engelhorn Centre in Mannheim, Germany, where they have been graphitized and dated (Kromer *et al.* 2013). The three dates from MPI were corrected for a residual preparation background estimated from pretreated ^{14}C free bone samples, kindly provided by the ORAU.

The radiocarbon results are listed in Table S6 (attached as Excel File). Burial 14 was dated twice at Beta laboratory, but unfortunately, the ages are statistically incompatible. We cannot discard one of the two dates, because not enough information about the collagen preservation is available. Until a third date is produced with more accurate and detailed information we will consider them not to be reliable, and for this reason, they are not included in the Bayesian model (see below). Burial 17 has one date from the adult individual and one date from the sub-adult individual. The two ages are compatible according to the R_Combine function of Oxcal (Burial 17, R_Combine, ^{14}C Age 8,620±36).

Based on the distribution of radiocarbon dates (Fig. 3b) it is clear that they cluster into three distinct groups roughly corresponding to the early, mid and late Holocene. From this initial assessment, the radiocarbon dates were calibrated using the SHcal13 (Hogg *et al.* 2013) curve and modelled into three contiguous phases using OxCal 4.2 (Ramsey & Lee 2013) (see Supplementary Data 1 for the OxCal script). Lapa do Santo

deposit has a very expressive anthropogenic component (see section 7 on formation processes) and all charcoals are assumed to derive from combustion structures. Discounted their *terminus post quem* nature, the charcoals from Lapa do Santo are themselves the events to be dated. Therefore, the t-type outlier model (Ramsey 2009) is not appropriate and instead we used a s-type outlier model (Ramsey 2009), with prior probabilities set at 0.05.

The agreement of this model is above the recommended threshold of 60% (A_overall = 82.1%). According to the utilized model Lapa do Santo's Period 1 (LSP-1) starts at 12.5 cal kyBP and ends at 8.1 cal kyBP, Lapa do Santo's Period 2 (LSP-2) starts at 5.2 cal kyBP and ends at 4.0 cal kyBP; Lapa do Santo's Period 3 (LSP-3) starts at 1.1 cal kyBP and ends at 0.7 cal kyBP (all 68.2% interval) (see light shaded areas in Fig. S2b). If we consider the 95.4% interval Lapa do Santo's Period 1 (LSP-1) starts at 12.7 cal kyBP and ends at 7.9 cal kyBP, Lapa do Santo's Period 2 (LSP-2) starts at 5.4 cal kyBP and ends at 3.9 cal kyBP; Lapa do Santo's Period 3 (LSP-3) starts at 2.1 cal kyBP and ends at 0.0 cal kyBP (see dark shaded areas in Fig. 3b)(Table S7). The chronology of Lapa do Santo will be based on these modelled calibrated ages.

According to the model two radiocarbon dates are outliers. The first is the oldest dated charcoal from the site (Beta-280489,^{14}C Age 10,490±50). However, we decided to keep this date in the model for two reasons. First, in Lagoa Santa region there is well-documented occupation at correspondent period testified by other sites (Araujo *et al.* 2012). Second, the oldest OSL dates of Lapa do Santo are roughly from the same timeframe as this charcoal. The second outlier is the date of Burial 11's collagen (Beta-215195,^{14}C Age 5,990±40). This date is chronologically intermediate between LSP-1 and LSP-2 and is considered an outlier if included in any of the two periods. Therefore, either Burial 11's date is to be discarded because it is incorrect, or because it represents an event of occupation that was not preserved in any other part of Lapa do Santo`s archaeological record. Taking into account the strong similarities Burial 11 shares with Burials 7 and 19, that date to more than a thousand years earlier, we favor the interpretation this is a wrong date that must be discarded.

The chronological range of each Lapa do Santo Mortuary Pattern (LSMP) was defined by the oldest extreme of the 95.4%interval of its oldest directly dated burial and the youngest extreme of the 95.4% interval of its youngest directly dated burial. Both burials from LSMP-1 could be directly dated resulting in a range of 9.7-10.6 cal kyBP

for this mortuary pattern. For LSMP-2 a total of six direct dates were obtained. Of those, two were discarded as not reliable (Burial 14) and two were combined since they referred to the same burial (Burial 17). LSMP-2 is dated to between 9.4-9.6 cal kyBP. For LSMP-3 a total of three direct dates on bone is available. Of those, one was discarded as an outlier (Burial 11). Based on the two remaining dates LSMP-3 is dated to 8.2-8.6 cal kyBP.

From the total of 61 radiocarbon dates included in the model 56 come from the main excavation area where the human remains were found (pink area in Fig. 2). Contrary to what is observed for the OSL dates (see previous section), in the main excavation area charcoals and burials from the different periods are not randomly vertically distributed. They are mostly restricted to specific vertical intervals, meaning absolute depth (i.e. z-values) and radiocarbon age are strongly correlated. In fact, in 93% of the cases (four out of 56; Burial 2 and the three charcoals indicated by blue and red arrows in Figure 3a-b) it is possible to correctly predict the chronological period to which a radiocarbon date belongs solely based on its vertical position. More specifically, radiocarbon dates located below the z-value of 0.137 belong to LSP-1, between 0.137 and 0.971 to LSP-2 and above 0.947 to LSP-3 (these are the limits indicated by the dotted and dashed lines in Fig. S2). Among the burials belonging to LSMP-1, LSMP-2 and LSMP-3 the highest z-value is 0.059 (Burial 13). Since this value is inferior to the limit of 0.137 separating LSP-1 from LSP-2 we estimated that all these burials belong to LSP-1.

As discussed in section 7 of this Supplementary Information, allochthonous raw material was used for lithic production since the beginning of the occupation of Lapa do Santo. However, as indicated by the histogram depicted in the Figure 6a, after Level 20 of Unit F13 allochthonous raw material disappears from Lapa do Santo archaeological record. Unit F13`s Level 20 has an average z-value of -2.738. We used the equation of a linear regression of z-value against calibrated radiocarbon dates for the charcoals in units F13 and G13 (Figure 6b). Those are the charcoals located closest to the lithic assemblage analyzed (Unit F13) and, therefore, most suitable to estimate their chronology. When the z-value -2.738 is applied to the equation of the linear regression a date of 9.9 cal kyBP is obtained with a 95% confidence interval going from 8.5 cal kyBP to 10.4 cal kyBP. However, the lower limit of this estimation must be seen as very conservative since it is heavily influenced by the presence of a single charcoal sample

that is younger than the others at corresponding depth (Beta-15924). In the future, a more appropriate chronological model for the different levels based on Bayesian statistics should be prepared to improve this estimation.

The same linear equation is also appropriate to present a conservative chronological estimation for the hematite axe, projectile point and two fish-hooks that were found in units F12, F13, G12 and G13 (see section 7 for a description of stone and bone artifacts).

3. Formation Processes

Here we present the preliminary results of micromorphological analyses from a second excavation area opened at Lapa do Santo in 2011. This area corresponds to the same levels where burials from LSMP-1, LSMP-2 and LSMP-3 were found. For the complete geoarchaeological study, the reader is referred to Villagran et al., (*in press*). A total of 30 undisturbed blocks for micromorphological analyses were taken from the exposed surfaces during excavation. The horizontal strategy of sample collection aimed at covering the lateral and vertical variation in the sedimentary facies described during excavation. The blocks were oven-dried for one week at 50º C and impregnated with a mixture of polyester resin (Viscovoss N5 S, 700 ml), styrene (300 ml) and hardener (MKEP, 5-7 ml). Analyses were done with a Stemi 2000-C stereomicroscope and Zeis Axio Imager A2 petrographic microscope in plane polarized light (PPL), and cross-polarized light (XPL). Samples were prepared and analyzed at the Institute for Archaeological Sciences, Eberhard Karls Universität Tübingen.

The macro stratigraphy of Lapa do Santo shows an intercalation of layers with diffuse to sharp boundaries that can be divided into three main categories, from more to the less frequent: 1) tabular, grey, centimetric layers (5YR 6.1) of powdery carbonate sediments, with common sand grains and frequent to common red clay aggregates and charcoal (20-40 %); 2) lenticular, red centimetric layers (5YR 5.6) of indurated clay minerals with rare charcoal fragments; 3) lenticular, black, milimetric and centimetric layers, with high concentration of charcoal and microcharcoal.

Of the 30 thin sections analyzed, 27 show a similar composition characterized by: 1) coarse fraction made of randomly distributed clay aggregates of diverse size (from 30 µm to 1 cm) (Fig. 4a); 2) micromass made of densely packed ash crystals (Fig. 4b-c).

The remaining 3 thin sections are exclusively red clayey sediments (2 samples) and a fragment of limestone from the cave walls (1 sample). Differences between the samples are observed by variations in the c/f ratio, seen as changes in the relative frequency of ash crystals vs. clay aggregates. Other differentiating features are: porosity; frequency of organic elements, such as charcoal, articulated ashes (Fig. 4d) or tissue residues (Fig. 4e); and the presence of micro-stratifications (several microfacies in one sample) vs. samples made of one single microfacies.

Ash crystals are described as rhombohedric micro-crystalline calcite crystals (10-30 μm) (Fig. 4b). They develop from heating the calcium oxalates that naturally appear in the plant cells at temperatures around 400-600º C. Ash crystals, also described as pseudomorphs of calcium oxalate into calcite (POCC), are the diagnostic micromorphological trait of plant ashes (Canti 2003; Brochier 1983; Courty *et al.* 1989). The ash crystals at Lapa do Santo have an overall good preservation, with few areas if recrystallized ashes. Sparitic coatings and infillings, inside voids, around coarse fraction components and also cementing the ashes, suggest water passage through the sediments and vadose conditions, with slow water percolation and/or episodes of water saturation. The iron (hydr)oxide hypocoatings and nodules also indicate this.

The clay aggregates are always blocky, angular to sub-rounded, with undifferentiated b-fabrics (XPL). They appear in frequencies from 10-70% and show four distinct colors in PPL: red, orange, yellow and dark brown. The differences could be related to differences in the iron content or to anthropic modifications (e.g. human fires) as suggested by the dark red rims (Fig. 4f). The microstructure inside the clay aggregates is close granular to massive, with star-shaped voids (from coalesced granules), chamber voids (from biological activity) and fissures. Laminated clay coatings and infillings were observed inside the clay aggregates, suggesting provenance from B_t horizons. Very fine sand and fine sand sub-rounded quartz grains are embedded in the clay aggregates (frequency below 5%), with random distribution and good selection.

The coarse fraction is also made of other organic and inorganic components that appear in concentrations below 5%, such as: limestone fragments (from the cave walls); microlithic flakes; opaque minerals and quartz grains (detached from the clay aggregates); bone fragments (sometimes burned); shell fragments; charcoal; articulated ashes; tissue residues; and phytoliths. Besides the ash crystals, the micromass also includes pale yellow (PPL), undifferentiated or low birefringence (XPL) material

possibly derived from neoformed phosphates. Given the low amount of bones in the sediments and the good conditions for bone preservation in the deposit (alkaline pH), phosphates could derive from bird guano and/or plant decay. The common association of phosphate layers with tissue residues, silicified tissue and plant pseudo-voids in numerous thin sections suggest that at least some portion of the secondary phosphates derives from plants.

Bioturbation is indicated by channel and chamber voids and few passage features. However, bioturbation was not intense since fragile components, such as tissue residues, laminations of fine plant tissue and articulated ashes show good integrity.

The mixing of geogenic (clay aggregates) and anthropogenic sediments (ashes) seen in Lapa do Santo is a frequent characteristic in rockshelters of Lagoa Santa. Ashes from anthropic fires have been described in the sediments of Lapa das Boleiras (Araujo *et al.* 2008) and Lapa Grande de Taquaraçu. Although no micromorphological analysis have been done in other sites, the macroscopic and micromorphological similarity between the greyish fine sediments in Lapa do Santo, Lapa das Boleiras and Lapa Grande de Taquaraçu indicate that plant ashes could be a frequent component in other archaeological sites in rockshelters from the region.

Geogenic clay aggregates making up the site stratigraphy and frequently mixed with plant ashes have also been reported at the Sumidouro cave (Piló *et al.* 2005) and Lapa das Boleiras (Araujo *et al.* 2008). At the Sumidouro cave, red and yellow sediments were interpreted as soil aggregates from the oxisol developed from the Serra de Santa Helena Formation (Araujo *et al.* 2005). At Lapa das Boleiras the clay aggregates are described as red colluvium derived from the red oxisols in the vicinity of the sites (Araujo *et al.* 2008).

The micromorphological characteristics of the clay aggregates in the sediments at Lapa do Santo also fit to what is described for the local red and yellow oxisols, such as: microstructure made of coalesced granules; and 1-5% frequency of very fine to fine sand sized quartz grains. The lack of cracks and conduits naturally bringing soil material to the rockshelter favors the interpretation that soil material came from the oxisol developed over the limestone shelter. Soil material loosened by rain, plant-root etc. continuously fell down the cliff above the rockshelter and was later redistributed by human trampling within the site and mixed with the ashes from combustion features. Spectroscopic studies indicate that more than half of the clay aggregates at the site have been affected by heating at temperatures above 600º C (see Villagran et al., in press).

4. Diatom analysis

Diatom analyses were done to investigate the potential flooding of the site by a pond that existed north of the rockshelter, and whose presence is indicated by watermarks in the limestone wall. Analyses were done on loose sediments collected in aseptic conditions from the second excavation area.

For the identification of siliceous microfossils 12 samples of loose sediment were dried in an oven at 40^{o}C. One gram of sample was placed in a 250 ml beaker, with 30 ml of hydrochloric acid to remove the carbonates. The solution was warmed on a hot plate for six hours under 100^{o}C. After carbonate removal, 30 ml of hydrogen peroxide were added to remove organic matter. Samples were successively rinsed with distilled water and decanted six times until solution reached a neutral pH. Afterwards, samples were diluted to 100 ml and 3 ml of the solution placed on a microscope slide and mounted with Nafrax.

Diatoms were identified in 70% of the analyzed samples but at a very low frequency. Eunotia, a genus generally preferring marshes, rivers, and lake habitats were the most common type of diatom. The genus lives in epilithic habitats (attached to rocks) in rivers and springs at a pH of 4.3 (slightly acid water), at water temperature of 26.3^{o}C, variable concentration of dissolved oxygen (2-10 mg/L), and null turbidity and salinity (Burlinga et al., 2007). *Hantzschia amphioxis* was also identified. It inhabits temporal bodies of water or periodically emerging areas associated with ephemeral drainage channels (Camburn et al., 2010). Although the assemblage is compatible with a lacustrine environment, the very low frequency of diatoms observed in the sediments indicates that diatoms were not deposited by a permanent or seasonal water body . However, the presence of reworked diatoms, frustules and sponge spicules suggest some sort of water input to the site, possibly brought to the site by its dwellers from the nearby lakes. Future work characterizing diatom assemblages in other locations in Lagoa Santa will allow a more precise interpretation of the diatoms assemblage at Lapa do Santo.

5. Zooarchaeology

Zooarchaeological analyses are key to better understand the relationship between humans and other animal populations, specifically for studies on diet and hunting strategies (Reitz & Wing 2008). A central point, however, is how we can interpret the zooarchaeological record to generate unbiased information about those relationships. Wrong interpretations can derive from the incorrect understanding of the role that human and natural agencies play in constituting the faunal assemblage recovered in archaeological sites (Lyman 1994; Kipnis 2002; Bissaro Jr. 2008; Perez 2009).

For the faunal analyses at Lapa do Santo we followed standard zooarchaeological methodology (Klein & Cruz-Uribe 1984; Lyman 1994; Lyman 2008). The Number of Identified Specimens (NISP) and Minimum Number of Individuals (MNI) was computed for a sample of faunal assemblage coming from units: L7, L8, L10, M3, M4, M5, M6, and from archaeological strata contemporary to the early Holocene human remains. The results point to a faunal assemblage dominated by small and medium-sized mammals, as well as reptiles, birds and fishes (Table S8). Bigger mammals, such as deer and peccaries are also present in the faunal assemblage, but not as predominantly as one would expect based on their much higher return rate when compared to medium-sized animals; but in accordance with evolutionary ecology models for prehistoric foraging societies in Central Brazil (Kipnis 2002).

The fact that almost all the anatomical parts of deer are represented (Table S9) indicates a subsistence/dietary strategy that is not targeting specific body parts when analyzed against Food Utility Index (Metcalfe & Jones 1988) (FUI). The game was not dismembered in the killing site, but brought as entire piece to the dwelling camp (see examples on the use of utility index in Binford (1978), Brink (1997), Brink and Dawe (1989), Lyman *et al.* (1992), Metcalfe and Jones (1988), Savelle *et al.* (1996), Savelle and Friesen (1996), Kipnis (2002); Fernández-Jalvo *et al.* (2002), Denys (2002), Bissaro-Júnior (2008), Couso *et al.* (2011), Manne (2014)).

However, the signature of hunting strategies based on Food Utility Indexes can be biased by the differential weathering of bones with varying densities (Rogers 2000). To verify if the anatomical representation of *Mazama* sp. in Lapa do Santo is reflecting dietary/hunting practices, instead of resulting from taphonomic processes, we evaluated the differential preservation of *Mazama* sp. bones according to density-mediated attrition (Grayson 1989; Lyman 1985; Lyman 1992).

For that, taphonomic signatures of natural and human agency were generated from paleontological and ethnoarchaeological assemblages as control studies for comparing with the zooarchaeological record from Lapa do Santo (Bissaro Jr. 2008).

For the paleontological sample we used bones recovered from the Gruta Cuvieri, a paleontological site located few kilometers from Lapa do Santo, with similar chronology, and rich in bones of *Mazama* sp. Previous studies showed the lack of anthropic inputs in the formation of Gruta Cuvieri fossil record (Hubbe *et al.* 2011), making it an ideal control sample of a non-human-mediated assemblage. For the ethnoarchaeological samples, we used bones recovered by Renato Kipnis in the early 1990´s at a Guajá site. The Guajá is one of the last hunter-gatherers society of South America lowlands (Forline 1997). They live in Brazilian Amazon (state of Maranhão) and commonly hunt *Mazama* sp., among other species (for a detailed description of the Guajá subsistence strategy see Prado (2009)). The bones used in this study were collected after discard and were an ideal control sample for a human-mediated assemblage.

For the taphonomic study, deer bones from other excavated units at Lapa do Santo were also included as to have a more significant sample size. The relative skeletal abundance of *Mazama* sp. in Lapa do Santo, Gruta Cuvieri and the Guajá assemblage was quantified using the Standardized Minimum Number of Animal Unit (%MAU, Binford 1984) for each anatomical part. Because there are no specific utility indices for *Mazama* sp. the bone density of the body parts considered in this study was obtained from Lyman(Lyman 1984) reports on *Odocoileus virginianus* (Artiodactyla, Cervidae). Table S10 presents the correlation between %MAU and bone density for the three sites.

In the paleontological context (Gruta Cuvieri) the positive and significant correlation between %MAU and bone density supports the survivorship of higher density anatomical parts due to density-mediated attrition (e.g. post-depositional). The absence of any significant correlation between %MAU and bone density in the ethnoarchaeological assemblage (Guajá) indicates that whole deer skeletons were entering the Guajá settlement.

In Lapa do Santo, the non-significant correlation between %MAU of *Mazama* sp. and bone density indicates that density-mediated attrition was not central to the pattern observed. The low depositional rates at Gruta Cuvieri would have given enough time for density-mediated attrition to take place before the bones were completely buried, resulting in their differential preservation. In Lapa do Santo, however, the fast

depositional rates associated with anthropogenic sediments that contain high degree of ashes and calcium, good for bone preservation, would have precluded the differential preservation of the bone assemblage triggered by density-mediated attrition.

Thus, we interpret that the representation of bones in Lapa do Santo did not result from differential preservation, but is indeed reflecting a hunting strategy in which *Mazama* sp. was not dismembered in the killing site, but brought as an entire piece to the dwelling camp. This is supported by the lack of significant statistical correlation between %MAU and FUI for *Mazama* sp. in Lapa do Santo (n=25, *Spearman rho*=0.344; p=0.09). Similar values are observed for the Guajá ethnoarchaeological collection (n=27, *Spearman rho* = 0.268; p=0.17) attesting this is a common hunting strategy in the tropics, where even the largest game, tapir, can still be carried without dismembering (Kipnis 2002). In conclusion, the faunal assemblage from Lapa do Santo is an adequate sample upon which to base inferences about prehistoric human faunal exploitation, and that the inferences point towards a hunting strategy of small and medium-size animals as the primary prey items, and less frequent the inclusion of bigger animals upon encounter (Bissaro Jr. 2008; Kipnis 2002).

6. Carbon and Nitrogen Isotopes

Carbon and nitrogen stable isotope analysis on bone collagen is widely used in archaeology for reconstructing ancient diets (Vogel & van der Merwe 1977; van der Merwe & Vogel 1978). Since almost all of the carbon in the biosphere is fixed by autotrophs (DeNiro & Epstein 1978), stable carbon isotopic ratios ($^{13}C/^{12}C$) can distinguish between plants that fixate carbon using C_3 and C_4 photosynthetic pathways (O`Leary 1988). C_4 type plants are mostly grasses, such as maize, sorghum and sugarcane, which have $\delta^{13}C$ values ranging from -14 to -9‰. C_3 type plants comprise some grasses (e.g. oats, wheat, rice) and virtually all other non-grasses, have $\delta^{13}C$ values ranging from -35 to -20‰ (Deines 1980).

Stable nitrogen isotopes ($^{15}N/^{14}N$) accumulate throughout successive trophic levels in which primary producers (plants) have the lowest ratios and each subsequent level in the trophic chain is enriched in approximately 3-5‰ (Hedges & Reynard 2007; Minagawa & Wada 1984; Schoeninger & DeNiro 1984) in $\delta^{15}N$ values. Modern day

studies show that plants in the Brazilian savanna, in which Lapa do Santo is located, have $\delta^{15}N$ values that range from -5.0‰ to +7.9‰ (Bustamente *et al.* 2004).

Stable carbon and nitrogen isotope ratios can also be used to identify marine components in the diet. Marine organisms usually have a carbon enrichment, of the order of an increase of 7‰ in $\delta^{13}C$ since their primary source of carbon comes from dissolved bicarbonate (0‰) and not atmospheric CO_2 (-7‰) like terrestrial carbon fixers (Chisholm *et al.* 1982; Chisholm *et al.* 1983; Tauber 1981). Nitrogen also has enriched values in this context as marine trophic chains tend to be longer and leading to a more pronounced cumulative effect of $\delta^{15}N$ increase (Schoeninger & DeNiro 1984).

A total of 17 human bones and 51 faunal bones were processed. Due to poor preservation conditions only eight human (Table S9) and 22 faunal samples (Table S10) provided collagen with an acceptable C:N ratio between 2.9 and 3.6 (DeNiro 1985). Since the faunal material from Lapa do Santo was extremely fragmented and poorly preserved, with only seven reliable results, the assemblage was complemented with material from Gruta Cuvieri, a paleontological cave of compatible chronology located 3 km away from Lapa do Santo (A. Hubbe *et al.* 2011).

The material was analyzed in three different laboratories: the Dorothy Garrod Laboratory for Isotopic Analysis of the McDonald Institute for Archaeological Research, University of Cambridge (UC); the Laboratório de Ecologia Isotópica (Isotope Ecology Lab) at the Escola Superior de Agricultura Luis de Queirós, University of São Paulo (ESALQ-USP); and the isotope facilities at the Max-Planck Institute for Evolutionary Anthropology (MPI-EVA). This variation of laboratories also made for a slight difference in methodologies. As the data were produced in three different labs, there are differences in the methods employed.

The samples analyzed at the University of São Paulo (USP) and the University of Cambridge (UC) used the same collagen extraction methodology. Following Longin (1971), samples of bones ranging from 500mg to 1000mg were sandblasted using aluminium oxide and then demineralised in a 0.5M aq. solution of hydrochloric acid (HCl). Once demineralised, the bone material was rinsed 3 times in deionised water and gelatinized in a pH3 aq. solution at 75^{o}C for 48 hours. Then supernatant collagenous solution was removed from the test tube using an Evergreen Sera-Separa®, 4¼″ long, 9 ml capacity filter (4μm porosity) and freeze dried for 3 days. Once the collagen was dry,

individual samples were sub-sampled in triplicates of 0.7 to 0.9mg and finally sent to be analysed in the mass spectrometer. At the University of São Paulo samples were analysed in a Carlo Erba EA1100-CHN elemental analyzer coupled to a Thermo Finnigan Delta Plus isotope ratio mass spectrometer, while at the University of Cambridge they were run in a Costech elemental analyser coupled to a Thermo Finnigan MAT253 isotope ratio mass spectrometer. All results were calibrated with reference to international and laboratory standards. The samples analyzed in MPI-EVA were treated according the protocols of Talamo and Richards (Talamo & Richards 2011) that are described in detail in section 3. Figure S6b shows the results of all analyses.

Results for the fauna are mostly consistent with their dietary habits. Deer (*Mazama* sp.; Cervidae, Goldfuss 1820) are browsing animals, and in the savannas of central Brazil normally feed on more ^{13}C-depleted gallery forest plants (Marinho-Filho *et al.* 2002). Their predominantly C_3 plant based diet is compatible with the observed collagen $\delta^{13}C$ values of -20.7±1.6‰ and $\delta^{15}N$ values of 6.0±1.9 ‰ (1 sigma interval, n=10). The presence of an outlier (CvL2-6333) presenting high $\delta^{13}C$ values could be the result of incorrect taxonomic classification.

Tayassuidae (Palmer 1897) have generalist omnivore diets (Bodmer 1991; March 1993; Barreto *et al.* 1997). The total of 6 analyzed collagen samples clustered into two groups of three samples each. One group has a typical C_3 type herbivore diet, very similar to that found in deer, averaging $\delta^{13}C$ values of -22.5±1.0‰ and $\delta^{15}N$ values of 4.7±0.5‰; whilst the other group has a more carnivore-like diet, averaging $\delta^{13}C$ values of -16.5±1.0‰ and $\delta^{15}N$ values of 9.7±0.3‰. This difference could be due to a number of reasons such as their broad alimentary range, inter-species variation, environmental changes, or the small sample size.

Both armadillo species, *Dasypus novencinctus* and *Euphractus sexcinctus* (Dasypodidae, Gray 1821) are omnivores with a tendency to carnivory (Bezerra *et al.*; McDonough & Loughry 2003; Breece & Dusi 1985; McBee & Baker 1982). Both species have collagen isotope values compatible with a carnivorous behaviour: average $\delta^{13}C$ values of -14.9±1.7‰, and $\delta^{15}N$ values of 8.2±0.5‰ (n=3) and average $\delta^{13}C$ values of -18.4‰, and $\delta^{15}N$ values of 8.2‰ (n=2), respectively. These results might

seem unusually high, but similar ones have been found in armadillos from pre-classic Mayan sites (van der Merwe *et al.* 2000).

The human results are homogenous in their $\delta^{13}C$ values, displaying a mean of $\delta^{13}C$ -19.0±0.6‰, indicating a predominately C_3 based diet. The $\delta^{15}N$ values range from 5.3 to 11.3‰. The highest $\delta^{15}N$ value comes from an infant with non-erupted permanent dentition and probably reflects breastfeeding (Fuller *et al.* 2006) (blue disks in Figure 5a). Sub-adults with erupted permanent deciduous have $\delta^{15}N$ values more similar to adults (red disks in Figure 5a). The low $\delta^{15}N$ values in the adult population is distinct from the carnivores ($t=4.50$; $p=0.001$) and similar to the herbivores from Lagoa Santa region ($t=0.25$; $p=0.400$), suggesting a diet based on plants and supplemented by fauna (O'Connell & Hedges 1999). This is consistent with zooarchaeological studies from central Brazil pointing to a generalist diet mostly based on the gathering of plants but supplemented by small game (Kipnis 2002).

7. Lithic and bone technology

Lapa do Santo presents abundant lithic assemblage with tens of thousands of pieces collected. A complete study of this material is yet to be realized, but the content of Unit F13 was analyzed to offer a preliminary characterization. This unit is a good representative of the early Holocene phase of Lapa do Santo, presenting an approximately 4-m thick deposit of archaeological sediments that accumulated between 12.7-11.7 cal kyBP and 8.3-8.0 cal kyBP. A total of 3589 lithics were analyzed (Pugliese 2008). Of those 212 were plotted and 3377 recovered from the sieving. Among the plotted material, 84% are flakes (178), 11% cores (24) and the remaining 5% are composed of unused raw material, flaked pebbles, one hematite axe and one preform of a projectile point that based on its small size and the presence of a peduncle is assumed to be an arrowhead. This assemblage is dominated by small flakes and small cores and formal tools are very rare (see Figure S1 for selected examples of typical elements of Lapa do Santo industry). A total of 126 complete flakes were measured yielding the following average and standard deviation of length, width and thickness, respectively: 25.27±12.12mm; 21.18±9.66mm; 9.45±6.48mm.

There is almost no preparation of cores, and flakes were obtained by a reduction strategy resulting in 70% of amorphous cores. The flakes are rarely retouched (among

the 212 pieces, only one case was identified), but they sometimes present macroscopic use-wear traces. Flakes with and without macroscopic use wear have similar morphologies. It is proposed that the flakes were the final goal of the reduction strategy being used as instruments of some kind of specific activity such as cutting or scraping. It is proposed that the reduction strategy aimed for flakes with this morphological characteristics to be used directly for some kind of specific activity such as cutting or scraping without any further retouching. Experiments with crystal quartz flakes show they quickly become dull and since retouching is not observed it is assumed that they were used only a few times before being discarded (Pugliese 2008).

The lithic assemblage of Lapa do Santo has a low variability in raw material, forms and types. The incidence of curated vestiges is low and formal tools are virtually absent. Another characteristic of Lapa do Santo is the exhaustive exploitation of cores in which all planes of crystals are flaked. Altogether, this supports the hypothesis that specific activities were executed on the site (Binford 1982; Parry & Kelly 1987; Panja 2003). The constancy of the lithic types through time attests to the stability of the related activities and the efficiency of this technology. It is plausible that there is a strong correlation between the lithic industry and the processing of vegetables at Lapa do Santo, especially considering that this kind of vestige is very frequent at the site and that the characteristics of the used flakes indicate the potential employment of composite instruments for this sort of use (Pugliese 2008).

While lithic types were constant, the use of raw material varied through time (Fig. 6). Crystal quartz was by far the dominant raw material, but silex, quartzite and silicified sandstone also appears as a minor component during specific periods of occupation. Crystal quartz commonly occurs within the karstic region but the other three are allochthonous, being found in the vicinities of the karst in locations such as Jaboticatubas River (ca. 25 km) and Espinhaço Mountains (ca. 60 km). Silex, although scarcer and far easier to knap, was used in a similar way as crystal quartz, to produce flakes and cores. Thermal treatment of silex was common.

Although in low frequency, allochthonous raw material was used since the beginning of the occupation of Lapa do Santo (Unit F13, Level 40), but at approximately 9.9 cal kyBP (Fig. 6) it almost disappears from the site remaining present only at small quantities (see section on chronology for the basis upon which this date was obtained). The same pattern of drastic reduction in the use of exogenous raw material around 9.9 cal kyBP has been described in other sites in Lagoa Santa region,

such as the Lapa das Boleiras rockshelter (Araujo *et al.* 2008; Araujo & Pugliese Jr. 2010; Pugliese 2008) and also in open air sites in the Lagoa Santa region (A.G.M. Araujo *et al.* 2012). The abandonment of allochthonous raw material around 9.9 cal kyBP is interpreted as reflecting a shift towards a subsistence strategy more focused on local items immediately available in the karst. Taking into account how close to Lagoa Santa the sources of the allochthonous raw material were, if this interpretation is correct, it implies a very limited territorial range for these hunter-gatherer groups. This shift towards more expedient practices based on easily available raw material could imply a change in the mobility pattern related to the increased stability in the environment conditions with the advance of the early Holocene.

In addition to the tens of thousands of flakes and cores recovered from Lapa do Santo, one hematite "axe" blade (PN: Ls-6410; Fig. S2) and one projectile point (PN: Ls-5534; Fig. S3) were also found in the deposits belonging to LSP-1 (i.e. early Holocene). Other blades were found in Lapa do Santo but they are either not from the early Holocene component of the site or of unkown stratigraphic provenience and will not be described here. Even so, for sake of completeness we provide basic contextual information for all blades from Lapa do Santo in Table S14.

The piece identified with accession code St-6410 is the proximo-mesial part of a broken hematite 'axe'-blade and it weights 375g. It was found on level 31 of unit G13 of Lapa do Santo (x = 6.621, y = 12.726, z = -2.998, see the green diamond in Figures 2 and 3). It was recovered in August 2008. When this z-values is applied to the linear regression proposed in section 2 the estimated chronology for the hematite axe blade is 10.4 cal kyBP, ranging from 9.7 cal kyBP to 11.0 cal kyBP within a 95% parametric confidence interval.

The presence of knapping stigmas in the ventral face indicates this blade was produced from a thick flake and that it was most probably the head of an axe. Since no agriculture is known among the groups inhabiting Lagoa Santa during the early Holocene is unlikely this blade was the head of an adze (Fig. S2). The straight and planar breakage at the distal part is commonly observed in other blades from Brazil and is probably the result of a strong impact during use. The hematite blade from Lapa do Santo presents some polishing, mostly concentrated near the butt. The grinding seen in some parts of the artifact are the result of attrition with some vegetal material, probably the wooden shaft.

Both sides of the blade show technological signs of being produced over an anvil (Fig. S2). After the breakage, there was an attempt to reshape the blade, trough flaking the ventral side and using the flat broken surface as the striking platform. This process, however, was unable to properly reshape the blade, possibly leading to its abandonment/discard. The hematite blade from Lapa do Santo can be tentatively classified as cordiform following the typological scheme proposed by Prous et al., (2003). Cordiform blades are characterized by i) being completely bifacially flaked, ii) usually presenting the active edge narrower than the butt, iii) having an asymmetric beveled edge and, iv) presenting an aspect of an overall lack of aesthetic refinement. They contrast with the more symmetrical and fully polished axes blades that are more commonly found in Brazil.

Hematite blades are rare in Brazil. In the state of Minas Gerais (586,528 km^2), where Lapa do Santo is located, from a total of 155 known blades only 10 were produced over hematite (Ott 1958). The non-hematite blades are usually associated with ceramist occupations and are assumed to be more recent than those made over hematite (Souza 2013). However, this is a working hypothesis deserving further testing.

Among all hematite blades from Brazil only two were found in context: the one described in the present contribution and one from the archaeological site of Lapa das Boleiras (PN: Bl-2179)(see Araujo *et al.* 2008 for a detailed description of the site). Similar to the one from Lapa do Santo, the hematite blade from Lapa das Boleiras was found within the early Holocene component of the site. Although a sample size of two is far from enough to propose a general pattern, it seems that the hematite axe blades were a common element of the early Archaic tool-kit.

The findings from Lapa do Santo and Lapa das Boleiras support *Prous et al*., (2003) original suggestion that the so-called "cordiform blades" are related to the earlier periods of occupation in central Brazil. A third cordiform hematite blade was found in the site of Santana do Riacho (ca. 40 km from Lapa do Santo) and might belong to the early Archaic period as well. However, its chronology is ambiguous since it was found between layer 2 and layer 4 that are dated to 5.0-8.0kyBP and 8.0-10kyBP, respectively.

A detailed study on the provenience of the hematite used in Lagoa Santa region (i.e. Lapa do Santo and Boleira) is not yet available. The nearest known ferrous outcrop is located ca. 55 km to the south (the Cauê formation on the Curral Hills) but it might be possible that cobbles of hematite were available in the beds of the Velhas River, less

than 10km distant from Lapa do Santo. Therefore, it is not possible to be sure if the hematite was immediately accessible for the production of the blades or not.

Therefore, it is possible that the groups inhabiting Lagoa Santa during the early Holocene were intentionally targeting hematite as one of their favorite raw material for the production of axe blades. This might be explained by the greater hardness of hematite when compared to other raw materials commonly used for blade production and it has been shown (Souza 2013) that hematite blades have sharper cutting edges when compared to non-hematite blades. Besides, its red color and metallic shine can be considered as aesthetic appealing characteristics and, therefore, non-utilitarian reasons might explain the selection of hematite as raw material (Souza 2013).

The projectile point (PN: Ls-5534, Fig. S3) was recovered in July of 2002 in the level 28 of unit G12 (x=6.013, y=11.686, z=-2.673). When this z-values is applied to the linear regression proposed in section 2 the estimated chronology for the projectile point is 10.0 cal kyBP, ranging from 8.9 cal kyBP to 10.5 cal kyBP within a 95% parametric confidence interval. The projectile point is made out of silicified limestone, using a natural original plaque as a blank. It presents ground technique at one face. This is the most ancient evidence of the ground technique for lithic tools production (at reduction/*façonage* stage) in Americas to be recorded. The grounding technique is not usual for lithic points production in Brazilian industries, not even at Late Holocene. This projectile point has no technological similarity to the Early Holocene lithic points found at southern Brazil, related to the Umbu tradition industries (Moreno de Sousa 2014).

There are three possible explanation for the rare presence of these formal artifacts (i.e. hematite axe and projectile point): 1-) formal tools were commonly produced outside the rockshelters by the same groups that produced the flakes and cores commonly found in Lapa do Santo, but were almost never discarded within the rockshelters, 2) that groups with distinct lithic technology would eventually pass through Lagoa Santa or, 3-) that the groups from the karst were part of a broader socio-economic network and that these rare elements were obtained by some sort of interregional contact (Pugliese 2008). These are hypothesis deserving future investigation.

The bone artifacts from Lapa do Santo are very similar to what is observed in other parts of central Brazil during this chronological timeframe. A total of 198 bone artifacts or fragments of bone artifacts were found on the site, including spatulas (71%)

and burins (25%) (Fig. S4). Highly standardized and by far the most common type of artifacts occurring in Lapa do Santo, the spatulas' functions remain unknown. The manufacturing of these artifacts required considerable time investment and involved distinct types of techniques. The rare presence of elaborate fishhooks (six in total, Table S13 and Fig. S5) is at odds with the rare presence of fish remains at the site. All fishhooks were part of LSP-1. The fish hooks were all retrived from the sieve and therefore did not received a provenience number. Later in laboratory they received a special numeration from 1 to 6. Projectile points made from bone were not found on the site. Fifty-seven percent of the bone artifacts were made of deer bone, which was also by far the most commonly consumed animal in the site. A total of 49% of the artifacts were carved from metapodial deer bones (Santos 2011).

8. Microwear analysis of Lapa do Santo lithic

Archaeological artifacts function, within archaeological research, is often interpreted from its morphology. This creates a problem when dealing with archaeological assemblages which do not have formalized tools such as in Lapa do Santo. Microwear analysis offers a method to overcome such limitation by directly assessing the uses of lithic tools.

Properly conducted microwear research protocols involve three key steps: experimentation, blind testing, and analysis. Over the course of the previous four years one of the authors (HMR) has collected and created a collection of over 100 experimental tools. These tools were used for a broad range of activities including scraping, chopping, drilling, cutting, and butchery. Contact materials included wood, bone, antler, plant remains, animals, leather, hides, and shell. Microwear experiments are necessary in order to create comparative collections for use in analysis as well as for use in blind testing (Odell 1985; Tringham *et al.* 1974).

Blind tests are used to assess an analyst's preparedness for conducting work upon archaeological assemblages. These tests are conducted using experimental artifacts for whose use is known. Generally, ten to twenty experimental pieces are chosen by an outside party for the analyst to examine. Analysts must identify the location of utilization, relative action, relative hardness of contact material, exact action and exact contact material for each artifact selected in the examination. Scores are than calculated to determine the accuracy of the analyst. It should be noted that blind test scores often

underestimate the skills of an analyst. When examining archaeological assemblages, for any tool for which information is indeterminate analysts do not propose a guess, however when conducting a blind test analysts must put a precise answer to all questions, any blanks or indeterminate information is simply marked incorrect. This ensures that analyst cannot artificially inflate their scores by leaving blank answers but tends to negatively skew results. Scores for the most recent blind test for HMR are listed in Table S15.

In the course of analysis of archaeological collections, artifact uses are identified using a constellation of traits including edge scarring, striations, polish, and edge rounding. Since this analysis utilized primarily the low-power method, which utilizes magnification between 10-120x, edge scarring was of particular importance. Certain scar types, distributions, and sizes are associated with particular activities, which allow an analyst to identify both the action of the tool and the potential hardness of the contact material. For instance, a tool used in a longitudinal pattern will display scars on both edge surfaces, while a tool used for transverse activities will tend to have scarring on a single surface. The relative hardness of the contact materials also affects what kind of scars will be present, for instance use of softer materials, such as flesh or hides, tends to produce small scars, generally with feather terminations. Harder materials such as antler or bone will produce larger scars which often have step terminations and edge crushing. Comparisons with experimentally used pieces are vital during the course of analysis as some lithic raw materials will vary in the intensity of the edge scarring depending upon the brittleness of the raw material.

To explore the potential use of micro-wear analysis in the Lapa do Santo assemblage a sub-sample of nine lithics were chosen for a preliminary study. They were examined using a Nikon SMZ 800 microscope with a microscopic range of 10-120x magnification power. The nine lithic artifacts examined were made of quartz crystal which can be difficult to analyze due to its translucent crystalline structure. Artifacts were cleaned using water and toothbrush, a sonic cleaner was not utilized as quartz will occasionally break apart when subjected to this kind of cleaning. Some of the more stubborn soils were not removed as they were cemented to surface and their removal may have caused damage to the surface of the tool. When necessary powderized-paint was applied to the surface of the artifacts to improve the visibility of scar patterns, all artifacts were washed again after examination to remove all residue from the surface application.

From a total of nine analyzed lithics only one had definitive evidence of utilization that could be detected by microwear analysis. This lithic (St-7865) was recovered *in situ* on the 7th of May 2012 from Unit O3, Level 3, Facies 4. Its exact location within the excavation unit is x=14.325, y=2.154, z=0.416. The utilized piece is a small flake made on translucent crystal quartz, measuring 33.15mm long, 18.70mm wide, and 6.88mm thick. St-7865 has light utilization on polar coordinate seven. The scar patterns are bifacial and close together including scaler and feather scars and some snap fractures (Fig. S6a). The scars are small indicating the artifact was used as cutting implement of soft materials (Fig. S6b). Given the entire lack of polish development and striations it was not possible to assign a more exact material. Soft materials might include vegetal, hides, meat, cordage or grasses.

9. Strontium Isotopic data

Strontium isotopic analysis ($^{87}Sr/^{86}Sr$) of skeletal material is a commonly employed method for detecting provenance and mobility amongst mammals, including humans (Price *et al.* 2002; Price *et al.* 2004), because tooth enamel from individuals record the isotopic signal of when it is formed during the earliest stages of life (Humphrey *et al.* 2008). Since radiogenic isotope ^{87}Sr forms by radioactive decay from rubidium (^{87}Rb), the $^{87}Sr/^{86}Sr$ signature of a specific location is determined by the underlying bedrock age and its content of Rb. Younger geological formations like volcanic rocks have lower $^{87}Sr/^{86}Sr$ values than older geological formations such as granite. A specific geological strontium signature is incorporated into body biominerals by substituting for calcium (Ericson 1985; Price *et al.* 2002; Bentley 2006), since strontium enters the ecosystems with little or no fractionation (Faure & Powell 1972; Graustein 1989). Amongst skeletal tissues, to date, tooth enamel is the preferred substrate for this analysis, due to its greater resistance to diagenesis in the burial environment (Budd *et al.* 2000; Hoppe *et al.* 2003). Within a single archaeological population, $^{87}Sr/^{86}Sr$ analyses of individuals' teeth can potentially detect those who were born on differing geological substrates ("non-locals"). However, environmental background studies are needed to assess the local bioavailable $^{87}Sr/^{86}Sr$ signature from the different geologies in the study region (Price *et al.* 2002; Evans *et al.* 2010), in order to assess possible provenance and territorial mobility.

The human teeth were prepared in solution and analysed in a MC-ICP-MS for strontium isotope in the lab facilities of the Department of Human Evolution from the Max-Planck Institute for Evolutionary Anthropology (MPI-EVA) in Leipzig, Germany (Copeland *et al.* 2008). Solid pieces of enamel weighing approximately 20 mg were drilled from the crown of each of the teeth, spanning from the cement-enamel junction to the occlusal surface, and cleaned thoroughly on all sides under a magnifying lens with a diamond drill bit to ensure no dentine or other material remained attached to it. After the drilling and cleaning, the pieces of enamel were sonicated for at least 15 minutes in high purity deionized water, before they were taken to the MPI-EVA clean lab facility (PicoTrace GmbH, Bovenden, Germany). The samples were then rinsed three times with high purity deionized (18.2 MΩ) water (Milli-Q® Element A10 ultrapure water purification system, Millipore GmbH, Schwalbach, Germany), rinsed once with ultrapure acetone (GR for analysis grade, ≥ 99.8 %, Merck KGaA, Darmstadt, Germany), and dried overnight.

Further preparation of the enamel samples followed a modified version of the method described by Deniel and Pin (Deniel & Pin 2001). Each enamel sample was weighed into clean 3 mL Savillex^{TM} (Minnetonka, MN, USA) vials and closed-vessel digested on a heating block at 120 ºC in 1 mL of 14.3M nitric acid (HNO_3) before being evaporated to dryness at around 90-120 minutes. The resulting residue was then re-dissolved in 1 mL 3M HNO_3 in order to pass its solution through ion exchange chromatography using 50-100 μm bead size Sr-spec^{TM} resin (EiChrom Technologies, Inc., Darien, USA) suspended in ultrapure deionized water(Horwitz *et al.* 1992) and previously cleaned following the procedure delineated by Charlier and collaborators (Charlier *et al.* 2006). Several washes were carried out with 3M HNO_3 before the Sr in the sample was eluted with ultrapure deionized water, dried down, and redissolved in 3% HNO_3 prior to MC-ICP-MS analysis.

A standard with known strontium isotope values (Bone Meal SRM 1486, National Institute of Standards & Technology, USA) and a blank sample were prepared parallel to the samples. Thus, one preparation batch was formed by 13 samples, 1 standard, and 1 blank. All acids used were made from SupraPur® grade (Merck KGaA) stock solutions and diluted using ultrapure deionized water.

A Thermo Fisher Neptune^{TM} (Thermo Fisher Scientific Inc., Dreieich, Germany) MC-ICP-MS instrument at the MPI-EVA facilities (see Table S16 for operational

parameters) was used to obtain the strontium isotope measurements. This mass spectrometer is a high-resolution double-focusing one, equipped with nine Faraday detectors fitted with 10^{11} Ω resistors (four movable detectors H1-H4/L1-L4 on either side of a fixed axial detector) and a Virtual Amplifier^{TM} system which eliminates possible amplifier-detector bias and provides a dynamic range of 5 mV to 50 V on each detector (Batey *et al.* 2005; Nowell *et al.* 2003). A 100 μL/min self-aspirating capillary and MicroFlow PFA (perfluoroalkoxy) ST-nebulizer (Elemental Scientific Inc., Omaha, USA) was used to introduce the solutions, diluted in 3% HNO_3 to give ^{88}Sr signal intensities of 20-25 V into the plasma.

A static mode using a collector configuration similar to that described by Batey and collaborators (Batey *et al.* 2005) was used to measure $^{87}Sr/^{86}Sr$ strontium isotope values. The analysis of each sample was divided in two consecutive parts: a first baseline measurement at half mass positions (85.6 and 86.5) of the axial cup mass (^{86}Sr) for 30s (20 cycles each 1.05 s), and secondly data collection involving a block of 50 cycles of 2 s integrated time. Interferences by Kr in the carrier gas (argon) and by Rb in both the carrier gas and samples were corrected, same as mass bias normalization (using $^{88}Sr/^{86}Sr$=8.375209, exponential law), following an inverse mass bias correction procedure described by Nowell and collaborators (Nowell *et al.* 2003).

A regression equation described by Copeland and collaborators (Copeland *et al.* 2008) was used for estimating the strontium concentration (ppm) of the enamel solution runs, based on the ^{88}Sr signal intensity (V) of three solutions with known strontium concentrations (100, 400 and 700 ppb). We used the strontium carbonate isotopic standard SRM 987 (NIST, USA)SRM 987as working standard during the measurement, standard SRM 1486 as prepared external standard, and blanks as controls for contamination during the preparation. Thus, one analytical session was composed of 24 samples, 2 prepared blanks, 2 prepared standards SRM 1486, and 8 working standards SRM 987 with 16 blanks (one before and one after the working standard). Samples of this study were measured in two different analytical sessions.

Repeated $^{87}Sr/^{86}Sr$ measurements of working standard SRM_987 resulted in a mean of 0.710287 ± 0.000010 (1σ, n=16) during the analytical sessions and were corrected to the accepted value of 0.710240 ± 0.00004 (Terakado et al., 1988; Johnson et al., 1990). The long-term average for $^{87}Sr/^{86}Sr$ of the external standard SRM 1486 is 0.709297 ± 0.000024 (n=68). The measurements of standard SRM 1486 resulted in a

mean of 0.709297± 0.000011 (1σ, n=2) during the analytical sessions. All procedural blanks were considered negligible (^{88}Sr < 0.040 V) at <0.4% of the analyte signal intensity (^{88}Sr= ≈20V).

To provide a preliminary background of the local level of strontium bioavailability in Lagoa Santa region forty-two shell samples from Lapa do Santo and 34 shell samples from Lapa das Boleiras (A.G.M. Araujo *et al.* 2008) were also analyzed. Geologically Lagoa Santa region is fairly homogeneous being largely dominated by late Neo-Proterozoic sedimentary rocks (see section 1). Therefore, the level of strontium bioavailability is not expected to vary widely within the region. These samples were prepared and analysed in the lab facilities of the Universidade de Brasília, in Brasília, Brazil. The mechanical cleaning was done with a brush with soft plastic bristles to remove superficial impurities and then followed by ultrasonic cleaning during 5 minutes in ultra-pure water. After this step, the samples were dried down in an oven at room temperature. The chemical cleaning involved 3 different sequences of rinsing operations to remove any organic remains: diluted peroxide oxygen (H_2O_2), 0.1M glacial acetic acid and ultrapure water. In the case this treatment was not enough to fully dissolve the sample they were further subjected to 0.1M hydrochloric acid treatments during a few seconds. After being dried, the fragment was grinded manually using agate mortar and pestle. Usually, aliquots of 0.3 to 20 mg of powdered samples were used depending on sample availability.

The Sr for isotope analysis was separated using Teflon Eichrom microcolumns with specific Sr resin (EiChrom Technologies, Inc., Darien, USA) after it was dissolved using 500 µl of 5N HNO_3. The separated Sr was dissolved using 5ml of 3% nitric acid and the isotopic composition of strontium was determined on an MC-ICP-MS (Neptune from Thermo Instruments) in the Laboratory of Geochronology of Universidade de Brasília. The concentration of Sr in the solution was usually higher than 200 ppb, allowing it to minimize the isobaric interferences from Kr which are always present in the Argon gas necessary to cool the plasma source. The $^{87}Sr/^{86}Sr$ ratios were corrected for isotope fractionation to $^{88}Sr/^{86}Sr$ =0.1194, as is currently adopted when using the thermal ionization mass spectrometry. The SRM 987 Sr isotope standard was analyzed 20 times and routinely interspersed every 5 samples in the course of this analysis. Its average value and standard deviation were 0.710300 and 0.0000013, respectively. Since this value is slightly higher than the expected 0.710248 described by

McArthur(McArthur 1994), all sample ratios were corrected by subtracting a fixed value of 0.000052.

Strontium $^{87}Sr/^{86}Sr$ values from the 23 enamel samples (Table S17) were successfully measured. The $^{87}Sr/^{86}Sr$ ratio measured in human enamel has a mean value of 0.722 ± 0.005 (1σ) and ± 0.001 (2σ), with minimum and maximum values of 0.717 and 0.739 respectively. The values of all but one, Burial 10 (0.739), fall well within the 2σ mean value of the population (Figure S5b). Burial 10 is the only one that was cremated and this could explain its anomalous behaviour by indicating that the individual in it buried was an outlier coming from terrains presenting higher $^{87}Sr/^{86}Sr$ values. This suggests that the majority of the individuals lived on a same type of terrain, at least during the major time of the crown formation of their respective analysed teeth: P4 (n=11, 6-7 years old), M2 (n=2, 7-8 years old), M3 (n=2, variable, normally during early adulthood) and deciduous M2 (n=8, 10 months; if breastfed, representing their mothers' values). Furthermore, these values are close to the bioavailable strontium signature of the region, as indicated by the analysis of the 76 shells. Together, this is compatible with a scenario of low territorial mobility and a subsistence strategy probably based on local items. Future studies focusing on better characterising the strontium bioavailability within Lagoa Santa and nearby regions will further improve our capacity of understanding the significance of the Sr ratios reported here.

10. Cranial morphological affinities

The seven most complete adult skulls from Lapa do Santo (Burials 1, 5, 11, 14, 17, 21, 26) were measured by DVB following Howells protocol (Howells 1973; Howells 1989). The Lapa do Santo skulls were then compared to reference samples representing other Lagoa Santa populations (Cerca Grande (Neves *et al.* 2004) and Sumidouro (Neves, Hubbe, & Piló 2007)), Early and Archaic Colombia Series (Neves, Hubbe, & Correal 2007) and reference populations from Howells database (Howells 1996). Together they create an appropriate framework to interpret the morphological affinities between the Lapa do Santo Individuals and the morphological variation in the America across time in relation to the modern human worldwide cranial morphological variation (see Table S18 for details on the series included).The morphological affinities analyses were based on 22 variables (Table S19), selected to minimize a number of missing values among

the prehistoric individuals. The remaining missing values were replaced by means of multiple regressions (M. Hubbe *et al.* 2011). For all analyses, size was removed from the individuals by calculating a double z-score of the values (Relethford 1994; Neves *et al.* 2013).

To explore the morphological affinities of the series, we realized two analyses. First, Mahalanobis D^2 distances (Mahalanobis 1936) were calculated between series. The relationship between series given by the resulting matrix was then graphically represented through a Ward's Hierarchical Cluster (Ward Jr. 1963), which combine series into clusters that minimize within-cluster variation while maximizing between-cluster variation. To test the impact that subsampling has in the patterns of association between Lapa do Santo and the remaining series, the cluster was repeated 1000 times, each time on a different permutation with the original data, respecting the initial sample sizes. The frequency of times the same topologies occurred between each branch of the original cluster in each of the permutations was used as a measurement of the strength of the morphological associations between series. In other words, this indicates how well the average morphology obtained in a series represents the real morphological affinities of the population represented by the skull sample.

Second, morphological affinities were also represented in the first two Principal Components (PCs) extracted from the covariance matrix between series. PCs were calculated from the covariance matrix instead of the correlation matrix since the size correction procedure adopted here (see below) standardizes the variance of the variables to a large degree (Roseman & Weaver 2004). PC scores were calculated for all individuals in the dataset. To facilitate visualization, the individuals from Lapa do Santo were plotted together with the centroids of the series in a scatterplot based on the first two Principal Components. In this way, it is possible to compare results from a dimension reduction analysis (Principal Components Analysis), where only the major axes of variation between series are represented, with a distance matrix analysis (Wards Cluster), which considers the totality of the differences between the groups, weighted in this case by the covariance between variables.

Figure 7a (left) shows the results of the cluster analysis. Lapa do Santo appears in a cluster together with the other Lagoa Santa Series, the Colombians series, and Easter Island. The associations between this cluster are not very stable (p=0.50), however this cluster, in general, has strong affinities with the cluster composed by

Australo-Melanesians (p=0.90), which reinforces the idea that all Lagoa Santa groups share a common morphological pattern, similar to Australo-Melanesians and quite distinct from late Native Americans.

Figure 7a (right) shows the morphological affinities among the series based on the first two Principal Components, which together explain 29.1% of the original variation. The centroids, plotted in black, show a similar pattern of affinities from the one obtained by the cluster analysis. Lapa do Santo share the same position in the morphospace with other Lagoa Santa populations, the Colombian series, Australo-Melanesians, and Sub-Saharan Africans. However, in this analysis, the Lapa do Santo centroid appears closer to Australo-Melanesians and Easter Island, than to other Early South Americans series, which appear closer to the Sub-Saharan African series. Most of the Lapa do Santo individuals, plotted in red, share the same general morphology. The only exception is Burial 17, who appears as an outlier to the series, more closely associated to one of the Polynesia series (Moriori). The main difference between Early Americans and Late Americans is given by differences in the first Principal Component, which is positively correlated with cranial breadth (XCB) and total and midfacial height (NPH, NLH, OBH, WMH), and negatively correlated with cranial length (GOL, PAC, PAF). Therefore, series on the left side of the graph show longer and narrower neurocrania with relatively shorter faces, while series on the right side of the chart show the opposite pattern. The main difference between the Lapa do Santo centroid and the other early American series is due to the fact that Lapa do Santo tend to have wider orbits (OBB) and shorter Parietals (PAC, PAF).

In conclusion, the morphological analyses of the Lapa do Santo material show that they share the same morphological pattern with other Paleoamericans, which is quite distinct from the morphology shared by the Late Native Americans included in this analysis. This result is entirely consistent with previous studies of the Lagoa Santa material (Neves & Hubbe 2005; Neves, Hubbe, & Piló 2007; M. Hubbe *et al.* 2010). The one outlier (Burial 17) is hard to explain at this point, and future studies will have to address this individual for more details.

11. Estimation of sex and age at death

Sex estimation for Lapa do Santo skeletons was based on different anatomical regions: analysis of the skull (Walker 2008), the ischium-pubic region (Phenice 1969), the pelvis (Bruzek 2002), the proximal region of the ulna (Cowal & Pastor 2008), and the femoral diaphysis (Black 1978). These sex evaluations were done through a systematic study, by a single observer (Mariana Inglez). The observer tested her estimation skills in skeletons of the osteological collection of the Museum of Human Anatomy, at University of São Paulo, (MAH-USP), whose demographic profile is known. The accuracy of sex estimation varied from 74% for the femoral diaphysis to 85% for the pelvis (for details, see Inglez (2010). This range of accuracy is within those reported in the literature attesting the observer of the present study is properly skilled. The estimated sex and age at death for the individuals for Lapa do Santo are reported in Table S20. Although this particular publication focuses on the burials allocated to LSMP-1, LSMP-2 and LSMP-3 for the sake of completeness in Table S20 sex and age at death estimation is provided for all individuals from Lapa do Santo available at the date of this publication.

12. Supplementary references

AMBROSE, S.H. 1990. Preparation and characterization of bone and tooth collagen for isotopic analysis *Journal of Archaeological Science* 17: 431–51.

ARAUJO, A.G.M., J.K. FEATHERS., M. ARROYO-KALIN. & M.M. TIZUKA. 2008. Lapa das Boleiras rockshelter: stratigraphy and formation processes at a paleoamerican site in Central Brazil *Journal of Archaeological Science* 35: 3186–3202.

ARAUJO, A.G.M., W.A. NEVES. & R. KIPNIS. 2012. Lagoa Santa revisited: an overview of the chronology, subsistence, and material culture of paleoindian sites in eastern central Brazil *Latin American Antiquity* 23: 533–50.

ARAUJO, A.G.M., W.A. NEVES., L.B. PILÓ. & J.P. V. ATUI. 2005. Holocene dryness and human occupation in Brazil during the 'Archaic Gap' *Quaternary Research* 64: 298–307.

ARAUJO, A.G.M. & F. PUGLIESE JR. 2010. A Indústria Lítica, in A.G. de M. Araujo & W.A. Neves (ed.) *Lapa das Boleiras - Um Sítio Paleoíndio do Carste de Lagoa Santa, MG, Brasil*: 75–106. São Paulo: Anna Blume / FAPESP.

ARAUJO, A.G.M., A.M. STRAUSS., J.K. FEATHERS., J.C. PAISANI. & T.J. SCHRAGE. 2013. Paleoindian open-air sites in tropical settings: a case study in formation processes, dating methods, and paleoenvironmental models in central Brazil *Geoarchaeology* 28: 195–220.

BÁNYAI, M. 1997. *Minhas pesquisas arqueológicas na região de Lagoa Santa*. Symbiose.

BARRETO, G.R., O.E. HERNANDEZ. & J. OJASTI. 1997. Diet of peccaries *Journal of Zoology* 279: 279–84.

BATEY, J.H., T. PROHASKA., M.S.A. HORSTWOOD., G.M. NOWELL., H. GOENAGE-INFANT. & G.C. EIDEN. 2005. Mass Spectrometers, in *ICP Mass Spectrometry Handbook*: 26–116. Blackwell.

BENTLEY, R. 2006. Strontium Isotopes from the Earth to the Archaeological Skeleton: A Review *Journal of Archaeological Method and Theory* 13: 135–87.

BEZERRA, A.M.R., F.H.G. RODRIGUES. & A.P. CARMIGNOTTO. Predation of rodents by the yellow armadillo (Euphractus sexcinctus) in Cerrado of the Central Brazil *Mammalia* 65. Muséum national d'Histoire naturelle: 86–88.

BINFORD, L.R. 1978. Ethnoarchaeology *Archaeological Survey of Alberta Manuscript Series*.

— 1982. The archaeology of place *Journal of Anthropological Archaeology1* 1: 5–31.

BISSARO JR., M.C. 2008. Tafonomia como ferramenta zooarqueológica de interpretação: viés de representatividade óssea em sítios arqueológicos, paleontológico e etnográfico. Universidade de São Paulo.

BLACK, M.T. 1978. A new method for assessisng the sex of fragmentary skeletal remains: femoral shaft circumference. *American Journal of Physical Anthropology* 48: 227–31.

BODMER, R.E. 1991. Strategies of seed dispersal and seed predation in Amazonian ungulates 23: 255–61.

BØTTER-JENSEN, L. & V. MEJDAHL. 1988. Assessment of beta dose-rate using a GM multi-counter system *Nuclear Tracks and Radiation Measurements* 14: 187–91.

BREECE, G. & J. DUSI. 1985. Food habits and home range of the common long-nosed armadillo Dasypus novemcinctus in Alabama, in G. Montgomery (ed.) *The Evolution and Ecology of Armadillos, Sloths and Vermilinguas*: 419–27. Washington and London: Smithsonian institution Press.

BRINK, J.W. 1997. Fat Content in Leg Bones ofBison bison, and Applications to Archaeology *Journal of Archaeological Science* 24: 259–74.

BRINK, J.W. & B. DAWE. 1989. *Final report of the 1985 and 1986 field seasons at Head-Smashed-In Buffalo Jump, Alberta*. Archaeological Survey of Alberta.

BROCHIER, J.E. 1983. Bergeries et feux de bois néolithiques dans lê Midi de la France. Caractérisation et incendence sur lê raisonnement sédimentologique *Quartar* 33: 181–93.

BROWN, T.A., D.E. NELSON., J.S. VOGEL. & J.R. SOUTHON. 1988. Improved collagen extraction by modified Longin method *Radiocarbon* 30: 171–77.

BRUZEK, J.A. 2002. A method for visual determination of sex, using the human hip bone. *American Journal of Physical Anthropology* 117: 157–68.

BUDD, P., J. MONTGOMERY., B. BARREIRO. & R.G. THOMAS. 2000. Differential diagenesis of strontium in archaeological human dental tissues *Applied Geochemistry* 15: 687–94.

BUSTAMENTE, M., L. MARTINELLI., D. SILVA., P. CAMARGO., C. KLINK., T.

DOMINGUES. & R. V. SANTOS. 2004. 15N Natural abundance woody plants and soils of central Brazilian savannas (cerrado) *Ecological Applications* 14: 200–213.

CANTI, M.G. 2003. Aspects of the chemical and microscopic characteristics of plant ashes found in archaeological soils *CATENA* 54: 339–61.

CARTELLE, C. 1994. *Tempo passado: mamíferos fósseis em Minas Gerais*. Belo Horizonte: Editora Palco.

CHARLIER, B.L.A., C. GINIBRE., D. MORGAN., G.M. NOWELL., D.G. PEARSON., J.P. DAVIDSON. & C.J. OTTLEY. 2006. Methods for the microsampling and high-precision analysis of strontium and rubidium isotopes at single crystal scale for petrological and geochronological applications *Chemical Geology* 232: 114–33.

CHISHOLM, B.S., D.E. NELSON., K.A. HOBSON., H.P. SCHWARCZ. & M. KNYF. 1983. Carbon isotope measurement techniques for bone collagen: Notes for the archaeologist *Journal of Archaeological Science* 10: 355–60.

CHISHOLM, B.S., D.E. NELSON. & H.P. SCHWARCZ. 1982. Stable-carbon isotope ratios as a measure of marine versus terrestrial protein in ancient diets. *Science* 216: 1131–32.

COPELAND, S.R., M. SPONHEIMER., P.J. ROUX., V. GRIMES., J.A. LEE-THORP., D.J. De RUITER. & M.P. RICHARDS. 2008. Strontium isotope ratios (87 Sr / 86 Sr) of tooth enamel : a comparison of solution and laser ablation multicollector inductively coupled plasma mass spectrometry methods *Rapid Communications in Mass Spectrometry* 22: 3187–94.

COURTY, M.A., P. GOLDBERG. & R.I. MACPHAIL. 1989. *Soils and micromorphology in archaeology*. Cambridge: Cambridge University Press.

COUSO, M.G., R.A. MORALEJO., M.A. GIOVANNETTI., L.M. DEL PAPA. & M.C. PÁEZ. 2011. Inka occupation of enclosure 1- Kancha II, at El Shincal de Quimivil (Catamarca, Argentina) *Quaternary International* 245. Elsevier Ltd and INQUA: 159–69.

COWAL, L.S. & R.F. PASTOR. 2008. Dimensional variation in the proximal ulna: evaluation of a metric method for sex assessment *American Journal of Physical Anthropology* 135: 469–78.

DAVID, B., R.G. ROBERTS., J. MAGEE., J. MIALANES., C. TURNEY., M. BIRD., C. WHITE., L.K. FIFIELD. & J. TIBBY. 2007. Sediment mixing at Nonda Rock : investigations of stratigraphic integrity at an early archaeological site in northern Australia and implications for the human colonisation of the continent *Journal of Quaternary Science* 22: 449–79.

DEINES, P. 1980. The isotopic composition of reduced organic carbon, in J.C. Fontes (ed.) *Hand book of Environmental Isotope Geochemistry*: 329–406. Amsterdam: Elsevier.

DENIEL, C. & C. PIN. 2001. Single-stage method for the simultaneous isolation of lead and strontium from silicate samples for isotopic measurements *Analytica Chimica Acta* 426: 95–103.

DENIRO, M.J. 1985. Postmortem preservation and alterarion of in vivo bone collagen isotope ratios in relation to palaeodietary reconstruction *Nature* 317: 806–9.

DENIRO, M.J. & S. EPSTEIN. 1978. Influence of diet on the distribution of carbon isotopes in animals *Geochimica et Cosmochimica Acta* 42: 495–506.

DENYS, C. 2002. Taphonomy and experimentation *Archaeometry* 44: 469–84.

ERICSON, J.E. 1985. Strontium isotope characterization in the study of prehistoric human ecology *Journal of Human Evolution* 14: 503–14.

EVANS, J.A., J. MONTGOMERY., G. WILDMAN. & N. BOULTON. 2010. Spatial variations in biosphere 87Sr/86Sr in Britain *Journal of Geological Society* 167: 1–4.

FAURE, G. & T. POWELL. 1972. *Stontium Isotope Geology*. New York: Springer-Verlag.

FEATHERS, J., R. KIPNIS., L.B. PILÓ., M. ARROYO-KALIN. & D. COBLENTZ. 2010. How old is Luzia? Luminescence dating and stratigraphic integrity at Lapa Vermelha, Lagoa Santa, Brazil *Geoarchaeology* 25: 395–436.

FERNANDEZ-JALVO, Y., B. SANCHEZ-CHILLON., P. ANDREWS., S. FERNANDEZ-LOPEZ. & L. ALCALA MARTINEZ. 2002. Morphological taphonomic transformations of fossil bones in continental environments, and repercussions on their chemical composition *Archaeometry* 44: 353–61.

FORLINE, L.C. 1997. The persistence and cultural transformation of the Guajá Indians: Foragens of Maranhão State, Brazil. University of California.

FULLER, B.T., J.L. FULLER., D. a HARRIS. & R.E. HEDGES. 2006. Detection of breastfeeding and weaning in modern human infants with carbon and nitrogen stable isotope ratios. *American Journal of Physical Anthropology* 129: 279–93.

GALBRAITH, R.F. & R.G. ROBERTS. 2012. Statistical aspects of equivalent dose and error calculation and display in OSL dating: An overview and some recommendations *Quaternary Geochronology* 11. Elsevier B.V: 1–27.

GASCHE, H. & Ö. TUNCA. 1983. Guide to archaeostratigraphic classification and terminology: definitions and principles *Journal of Field Archaeology* 10: 325–35.

GRAUSTEIN, W.C. 1989. 87Sr/86Sr ratios measure the sources and flow of strontium in terrestrial ecosystems, in P.W. Rundel, J.R. Ehleringer, & K.A. Nagy (ed.) *Stable isotopes in ecological research*: 491–512. New York: Springer-Verlag.

GRAYSON, D.K. 1989. Bone transport, bone destruction, and reverse utility curves *Journal of Archaeological Science* 16: 643–52.

HANSEN, S. 1888. *En Anthropologisk Undersogelse af Jordfundne Menneskelevninger fra Brasilianske Huler. Med et Tillaeg om det Jordfundne Menneske fra Pontimelo*. La Plata: Rio de Arrecifes.

HEDGES, R.E. & L.M. REYNARD. 2007. Nitrogen isotopes and the trophic level of humans in archaeology *Journal of Archaeological Science* 34: 1240–51.

HIGHAM, T.F.G., R.M. JACOBI. & C.B. RAMSEY. 2006. AMS radiocarbon dating of ancient bone using ultrafiltration *Radiocarbon* 48: 179–95.

HOGG, A.G., - HUA QUAN., P.G. BLACKWELL., - MU NIU., C.E. BUCK., T.P. GUILDERSON., T.J. HEATON., J.G. PALMER., P.J. REIMER., R.W. REIMER., C.S.M. TURNEY. & S.R.H. ZIMMERMAN. 2013. SHcal13 southern hemisphere calibration, 0-50,000 years cal BP *Radiocarbon* 55: 1889–1903.

HOPPE, K.A., P.L. KOCH. & T.T. FURUTANI. 2003. Assessing the preservation of

biogenic strontium in fossil bones and tooth enamel *International Journal of Osteoarchaeology* 13: 20–28.

HORWITZ, E.P., R. CHIARIZIA. & M.L. DIETZ. 1992. A Novel Strontium Selective Extraction Chromatographic Resin *Solvent Extraction and Ion Exchange* 10: 313–36.

HOWELLS, W.W. 1973. Cranial variation in man: a study by multivariate analysis of patterns of difference among recent human populations *Papers of the Peabody Museum of Archaeology and Ethnology* 67.

— 1989. Skull shapes and the map *Papers of the Peabody Museum of Archaeology and Ethnology* 79.

— 1996. Howells' craniometric data on the internet *American Journal of Physical Anthropology* 101: 441–42.

HRDLÍČKA, A. 1912. Early Man in South America *Bureau of American Ethnology* 52.

HUBBE, A., P.M. HADDAD-MARTIM., M. HUBBE., E.L. MAYER., A.M. STRAUSS., A.S. AULER., L.B. PILÓ. & W.A. NEVES. 2011. Identification and importance of critical depositional gaps in pitfall cave environments: The fossiliferous deposit of Cuvieri Cave, eastern Brazil *Palaeogeography, Palaeoclimatology, Palaeoecology* 312. Elsevier B.V.: 66–78.

HUBBE, M., K. HARVATI. & W.A. NEVES. 2011. Paleoamerican morphology in the context of European and East Asian late Pleistocene variation: implications for human dispersion into the New World. *American Journal of Physical Anthropology* 144: 442–53.

HUBBE, M., W.A. NEVES. & K. HARVATI. 2010. Testing evolutionary and dispersion scenarios for the settlement of the new world. *PloS one* 5: e11105.

HUMPHREY, L.T., M.C. DEAN., T.E. JEFFRIES. & M. PENN. 2008. Unlocking evidence of early diet from tooth enamel. *Proceedings of the National Academy of Sciences of the United States of America* 105: 6834–39.

HURT, W. & O. BLASI. 1969. O Projeto Arqueológico Lagoa Santa – Minas Gerais, Brasil (nota final) *Arquivos do Museu Paranaense* 4: 1–63.

INGLEZ, M. 2010. Avaliação de métodos métricos e não métricos para assignação de sexo em esqueletos humanos. Universidade de São Paulo.

KIPNIS, R. 2002. Foraging societies of eastern central Brazil: an evolutionary ecology study of subsistence strategies during the terminal Pleistocene and early/middle Holocene. University of Michigan.

KLEIN, R.G. & K. CRUZ-URIBE. 1984. *The analysis of animal bones from archaeological sites – prehistoric archaeology and ecology*. Chicago: Chicago University Press.

KOLLMAN, J. 1884. Schadeln von Lagoa Santa *Z. Ethnol* 16: 194–99.

KROMER, B., S. LINDAUER., H.-A. SYNAL. & L. WACKER. 2013. MAMS – A new AMS facility at the Curt-Engelhorn-Centre for Achaeometry, Mannheim, Germany *Nuclear Instruments and Methods in Physics Research Section B: Beam Interactions with Materials and Atoms*. Elsevier B.V.

LAMING-EMPERAIRE, A. 1979. Missions archéologiques franco-brésiliennes de Lagoa Santa, Minas Gerais, Brésil – Le Grand abri de Lapa Vermelha *Revista de Pré-história* 1: 53–89.

LONGIN, R. 1971. New method of collagen extraction for radiocarbon dating *Nature* 230: 241–42.

LUNA, P. 2007. Peter Wilhelm Lund: o auge das suas investigações científicas e a razão para o término das suas pesquisas. Universidade São Paulo.

LUND, P.W. 1844. Notícia sobre ossadas humanas fósseis achadas numa caverna do Brasil, in P. Couto (ed.) *Memórias sobre a paleontologia brasileira*. Rio de Janeiro: Instituto Nacional do Livro.

LYMAN, R.L. 1984. Bone density and differential survivorship of fossil classes *Journal of Anthropological Archaeology* 3: 259–99.

— 1985. Bone frequencies: differential transport, in situ destruction, and the MGUI *Journal of Archaeological Science* 12: 221–36.

— 1992. Anatomical considerations of utility curves in Zooarchaeology *Journal of Archaeological Science* 19: 7–22.

— 1994. *Vertebrate Taphonomy*. Cambridge University Press.

— 2008. *Quantitative Paleozoology*. Cambridge University Press.

LYMAN, R.L., J.M. SAVELLE. & P. WHITRIDGE. 1992. Derivation and application of a meat utility index for phocid seals *Journal of Archaeological Science* 19: 531–55.

MAHALANOBIS, P.C. 1936. On the generalized distance in statistics *Proceedings of the National Institute for Science India* 2: 49–55.

MANNE, T. 2014. Early Upper Paleolithic bone processing and insights into small-scale storage of fats at Vale Boi, southern Iberia *Journal of Archaeological Science* 43. Elsevier Ltd: 111–23.

MARCH, I.J. 1993. The white-lipped peccary, in W. Oliver (ed.) *Pigs, Peccaries and Hippos*: 13–22. Gland: IUNC The World conservation union.

MARINHO-FILHO, J., F. RODRIGUES. & K. JUAREZ. 2002. . The Cerrado Mammals: Diversity, Ecology and Natural History, in *The Cerrados of Brazil: ecology, and natural history of a neotropical savanna*: 266–84. New York: Columbia University Press.

MAYYA, Y.S., P. MORTHEKAI., M.K. MURARI. & A.K. SINGHVI. 2006. Towards quantifying beta microdosimetric effects in single-grain quartz dose distribution *Radiation Measurements* 41: 1032–39.

MCARTHUR, J.M. 1994. Recent trends in strontium isotope stratigraphy *Terra Nova* 6: 331–58.

MCBEE, K. & R. BAKER. 1982. Dasypus novemcinctus *Mammalian Species, Northhampton* 162: 1–9.

MCDONOUGH, C. & W. LOUGHRY. 2003. Armadillos (Dasypodidae), in M. Hutchins (ed.) *Grzimek's Animal Life Encyclopedia*: 181–92. Farmington Hills: Thomson Gale.

METCALFE, D. & K.T. JONES. 1988. A reconsideration of animal body-part utility indices *American Antiquity* 53: 486–504.

MINAGAWA, M. & E. WADA. 1984. Stepwise enrichment of 15N along food chains: Further evidence and the relation between δ15N and animal age *Geochimica et Cosmochimica Acta* 48: 1135–40.

MORENO DE SOUSA, J.C. 2014. Cognição e cultura no mundo material: os Itaparicas, os Umbus e os 'Lagoassantenses'. Universidade de São Paulo.

MURRAY, A.S. & A.G. WINTLE. 2000. Luminescence dating of quartz using an improved single-aliquot regenerative-dose protocol *Radiation Measurements* 32: 57–73.

NEVES, W.A., R. GONZÁLEZ-JOSÉ., M. HUBBE., R. KIPNIS., A.G.M. ARAUJO. & O. BLASI. 2004. Early Holocene human skeletal remains from Cerca Grande, Lagoa Santa, Central Brazil, and the origins of the first Americans *World Archaeology* 36: 479–501.

NEVES, W.A. & M. HUBBE. 2005. Cranial morphology of early Americans from Lagoa Santa, Brazil: implications for the settlement of the New World. *Proceedings of the National Academy of Sciences of the United States of America* 102: 18309–14.

NEVES, W.A., M. HUBBE., D. BERNARDO., A.M. STRAUSS., A.G.M. ARAUJO. & R. KIPNIS. 2013. Early Human Occupation of Lagoa Santa , Eastern Central Brazil : Craniometric Variation of the Initial Settlers of South America, in K. GRAF, C. KETRON, & M. WATER (ed.) *Paleoamerican Odyssey*: 397–412. Texas A&M University Press.

NEVES, W.A., M. HUBBE. & G. CORREAL. 2007. Human Skeletal Remains From Sabana de Bogota Colombia : A Case of Paleoamerican Morphology Late Survival in South America ? *American Journal of Physical Anthropology* 133: 1080–98.

NEVES, W.A., M. HUBBE. & L.B. PILÓ. 2007. Early Holocene human skeletal remains from Sumidouro Cave, Lagoa Santa, Brazil: history of discoveries, geological and chronological context, and comparative cranial morphology. *Journal of Human Evolution* 52: 16–30.

NOWELL, G.M., D.G. PEARSON., C.J. OTTLEY., J. SCHWEITERS. & D. DOWALL. 2003. Long-term performance characteristics of a plasma ionisation multi-collector mass spectrometer (PIMMS): the ThermoFinnigan Neptune *Plasma Source Mass Spectrometry Spec Pub Royal Society of Chemestry*, 307–20.

NUNES, L., A. VICENTE. & D. CANDIDO. 2009. Tempo e clima no Brasil, in I. Cavalcanti (ed.) *Tempo e clima no Brasil*. São Paulo: Oficina de Textos.

O`LEARY, M.H. 1988. Carbon isotopes in photosynthesis *BioScience* 38: 328–36.

O'CONNELL, T.C. & R.E. HEDGES. 1999. Investigations into the effect of diet on modern human hair isotopic values. *American Journal of Physical Anthropology* 108: 409–25.

ODELL, G. 1985. On Evaluation of 'Blind Tests' in Lithic Use-Wear Research *Western Canadian Archaeologist* 2: 26–30.

OTT, C.F. 1958. *Pré-história da Bahia*. Salvador.

PANJA, S. 2003. Mobility strategies and site structure: a case study of Inamgaon *Journal*

of Anthropological Archaeology 22.

PARRY, W. & R.L. KELLY. 1987. Expedient core technology and sedentism, in J.K. Johnson & M. Morrow (ed.) *The organization of core technology*: 285–304. Boulder.

PEREZ, C.P. 2009. Paleoecologia de mamíferos viventes como ferramenta na caracterização do ambiente holocênico de Lagoa Santa, MG. Universidade de São Paulo.

PHENICE, T.W. 1969. A newlz developed visual method of sexing the Os Pubi *American Journal of Physical Anthropologyical Anhtropology* 30: 297–99.

PILÓ, L.B. 1998. Morfologia cárstica e materiais constituintes: dinâmica e evolução da depressão poligonal Macacos-Baú - Carste de Lagoa Santa, MG. Universidade de Sao Paulo.

PILÓ, L.B. & A.S. AULER. 2002. Apresentação: bicentenário de Peter Wilhelm Lund (1801-1880) *O Carste* 14: 4–7.

PILÓ, L.B., A.S. AULER., W.A. NEVES., X. WANG., H. CHENG. & R.L. EDWARDS. 2005. Geochronology, sediment provenance, and fossil emplacement at Sumidouro Cave, a classic late Pleistocene/early Holocene Paleoanthropological site in eastern Brazil *Geoarchaeology* 20: 751–64.

PRADO, H.M. 2009. O impacto da caça versus a conservação de primatas numa comunidade indígena Guajá. Universidade de São Paulo.

PRICE, T.D., J.H. BURTON. & R.A. BENTLEY. 2002. The characterization of biologically available strontium isotope ratios for the study of prehistoric migration *Archaeometry* 1: 117–35.

PRICE, T.D., C. KNIPPER., G. GRUPE. & V. SMRCKA. 2004. Strontium isotopes and prehistoric human migration: the Bell Beaker Period in Central Europe *Eurpopean Journal of Archaeology* 7: 9–40.

PROUS, A., M. ALONSO., H. PILÓ., L.A.F. XAVIER., A.P. LIMA. & G.N. SOUZA. 2003. Os machados pré-históricos no Brasil - descrição de coleções brasileiras e trabalhos experimentais: fabricação de lâminas, cabos, encabamento e utilização. *Canindé* 2: 161–236.

PUGLIESE, F. 2008. Os líticos de Lagoa Santa: um estudo sobre organização tecnológica de caçadores-coletores do Brasil Central. Universidade de São Paulo.

RAMSEY, C.B. 2009. Dealing with outliers and offsets in radiocarbon dating *Radiocarbon* 51: 1023–45.

RAMSEY, C.B. & S. LEE. 2013. Recent and planned developments of the program OxCal *Radiocarbon* 55: 720–30.

REITZ, E.J. & E.S. WING. 2008. *Zooarchaeology*. Cambridge University Press.

RELETHFORD, J.H. 1994. Craniometric variation among modern human populations. *American Journal of Physical Anthropology* 95: 53–62.

ROGERS, A.R. 2000. On equifinality in faunal analysis *American antiquity* 65. Society for American Archaeology: 709–23.

ROSEMAN, C. & T.D. WEAVER. 2004. Multivariate apportionment of global human

craniometric diversity. *American Journal of Physical Anthropology* 125: 257–63.

SANTOS, R.O. 2011. As tecnologias esqueletais: uma investigação sobre o uso de matérias-primas de origem esqueletal por meio de análise comparativa entre coleções arqueológicas e etnográficas. Universidade de São Paulo.

SAVELLE, J.M. & M.T. FRIESEN. 1996. An Odontocete (Cetacea) Meat Utility Index *Journal of Archaeological Science* 23: 713–21.

SAVELLE, J.M., M.T. FRIESEN. & R.L. LYMAN. 1996. Derivation and Application of an Otariid Utility Index *Journal of Archaeological Science* 23: 705–12.

SCHOENINGER, M.J. & M.J. DENIRO. 1984. Nitrogen and carbon isotopic composition of bone collagen from marine and terrestrial animals *Geochimica et Cosmochimica Acta* 48: 625–39.

SOUZA, G.N. 2013. Estudo das lâminas de pedra polidas do Brasil: diversidade regionais e culturais. Universidade de São Paulo.

STEIN, J.K. 1987. Deposits for Archaeologists *Advances in Archeological Method and Theory* 11: 337–95.

— 1992. *Deciphering a shell midden*. New York: Academic Press.

STEIN, J.K. & G.J. RAPP. 1985. Archaeological sediments: A largely untapped reservoir of information, in N.C. Wilkie & C.W.D. E. (ed.) *Contributions to Aegean archaeology*: 143–59. Minneapolis: Center for Ancient Studies, University of Minnesota, Publications in Ancient Studies 1.

TALAMO, S. & M. RICHARDS. 2011. A comparison of bone pretreatment methods for AMS dating of samples >30,000 BP *Radiocarbon* 53: 443–49.

TAUBER, H. 1981. 13C evidence for dietary habits of prehistoric man in Denmark *Nature* 292: 332–33.

TEN KATE, H. 1885. Sur les Crânes de Lagoa Santa *Bull. Soc. Anthropol.* 8: 240–44.

TRINGHAM, R.G., G. COOPER., G. ODELL., B. VOYTEK. & A. WHITMAN. 1974. Experimentation in the Formation of Edge Damage: A New Approach to Lithic Analysis *Journal of Field Archaeology1* 1: 171–96.

VAN DER MERWE, N., R. TYKOT., N. HAMMOND. & K. OAKBERG. 2000. Diet and animal husbandry of the preclassic Maya at Cuello, Belize: Isotopic and zooarchaeological evidence, in S. Ambrose & M. Katzmberg (ed.) *Biochemical Approaches to Paleodiatary Analysis*: 23–38. New York: Plenum Publisher.

VAN DER MERWE, N. & J.C. VOGEL. 1978. 13C evidence for dietary habits.

VAN KLINKEN, G.J. 1999. Bone Collagen Quality Indicators for Palaeodietary and Radiocarbon Measurements *Journal of Archaeological Science* 26: 687–95.

VIANA, H., H. KOHLER. & V. TAVARES. 1998. *Síntese da geologia, recursos minerais e geomorfologia. APA Carste de Lagoa Santa – MG*. Belo Horizonte: CPRM/IMABA.

VILLAGRAN, X., A.M. STRAUSS., C. MILLER., B. LIGOUIS. & R. OLIVEIRA. 2016. Buried in the ashes: formation processes of an early South American's site (Lapa do Santo, Brazil) *Journal of Archaeological Science*.

VOGEL, J. & N. VAN DER MERWE. 1977. Isotopic evidence for early maize cultivation in New York State *American Antiquity* 42: 238–42.

WALKER, P.L. 2008. Sexing skulls using discriminant function analysis of visually assessed traits *American Journal of Physical Anthropology* 136: 39–50.

WALTER, H. V. 1958. *Arqueologia da região de Lagoa Santa. SEDEGRA, Rio de Janeiro*. Rio de Janeiro: SEDEGRA.

WALTER, H. V., A. CATHOUD. & A. MATTOS. 1937. The Confins Man. A contribution to the study of Early Man in South America, in G.G. MacCurdy (ed.) *Early Man – As depicted by leading authorities at the international symposium the Academy of Natural Sciences Phyladelphia*. London: J. B. Lippincott Company.

WARD JR., J.H. 1963. Hierarchical grouping to optimize an objective function *Journal of American Statistical Association* 58: 236.

WINTLE, A.G. & A.S. MURRAY. 2006. A review of quartz optically stimulated luminescence characteristics and their relevance in single-aliquot regeneration dating protocols *Radiation Measurements* 41: 369–91.

13. Supplementary tables

Table S1: Basic information of the sediment samples.

Table S2: Concentrations relevant to dose rate.

Table S3: Dose rate information.

Table S4: Equivalent dose central age value and over-dispersion for each sample.

Table S5: Date and information on vertical position of the OSL samples from Lapa do Santo.

Table S6: Radiocarbon dates for Lapa do Santo (table available as a '.xls' file).

Table S7: Skeletal representation of *Mazama* sp. at Lapa do Santo.

Table S8: Correlations between skeletal abundance (%MAU) and bone density for *Mazama* sp.

Table S9: Human bone samples from Lapa do Santo analysed for carbon and nitrogen isotopes.

Table S10: Faunal bone samples from Lagoa Santa analysed for carbon and nitrogen isotopes.

Table S11. Contextual information of fishhooks found in Lapa do Santo.

Table S12. Contextual information of blades fishhooks found in Lapa do Santo.

Table S13: Blind Test Results for Heather M. Rockwell, administered December 2013.

Table S14: Operation parameters for MC-ICP-MS solution analysis used at the Max-Planck Institute for Evolutionary Anthropology (Leipzig, Germany).

Table S15: S-EVA number, archaeological code, $^{87}Sr/^{86}Sr$ ratio, $^{84}Sr/^{86}Sr$ ratio, Sr concentration (ppm) and voltage (^{88}Sr) from enamel of the human teeth prepared in solution and analysed in the MC-ICP-MS.

Table S16: Series included in the morphological affinity analyses.

Table S17: Craniometric measurements used in the morphological affinity analyses.

Table S18: Estimation of age at death for the skeletons of Lapa do Santo (table available as a '.xls' file).

Table S1: Basic information of the sediment samples.

Lab #	*OSL #*	*Year collected*	*Provenance*	*Depth from surface (cm)*
UW861	3	2002	Unit F13, red layer	132
UW1374	18	2005	Unit F13, red layer below hard white layer	164
UW1375	19	2005	Unit F13, red layer above whitish layer	92
UW1376	20	2005	Unit F13, red layer	27
UW1377	21	2005	Unit M6, above rocks at base of excavation	214

Table S2: Concentrations relevant to dose rate.

Sample	*^{238}U (ppm)*	*^{232}Th (ppm)*	*K (%)*	*Measured moisture (%)*
UW861	1.31±0.30	30.89±2.56	0.63±0.01	21.2
UW1374	2.72±0.25	17.52±1.66	0.71±0.02	13.7
UW1375	2.11±0.17	9.57±1.07	0.32±0.01	11.5
UW1376	2.31±0.24	17.52±1.67	0.28±0.01	14.1
UW1377	2.69±0.20	8.89±1.24	0.25±0.01	21.6
Rock below UW1374	0.47±0.04	0.20±0.15	0.02±0.01	-
White layer above UW1374	1.15±0.22	21.08±2.00	0.45±0.01	-
White layer near UW861	1.94±0.18	11.32±1.26	0.29±0.01	-
White layer below UW1376	2.23±0.19	9.27±1.26	0.24±0.01	-

Table S3: Dose rate information.

Sample	*ß dose rate (Gy/ka)*		*External dose rate (Gy/ka)*		*Total dose rate (Gy/ka)**
	ß-counting	*α-counting/flame photometry*	*dosimeter*	*laboratory*	
UW861	1.42±0.15	1.53±0.08			2.31±0.13
UW1374	1.38±0.12	1.43±0.06	0.94±0.03	1.05±0.07	1.97±0.07
UW1375	0.96±0.11	0.82±0.04	1.17±0.08	0.74±0.06	1.77±0.09
UW1376	1.31±0.20	1.03±0.06	1.02±0.11	1.03±0.08	1.90±0.10
UW1377	0.86±0.14	0.83±0.04			1.22±0.07

* Total dose rate reflects corrections for moisture content, which are not taken into consideration in the beta dose rates listed. The total dose rate also includes a small alpha contribution. It also depends on whether the dosimeter or laboratory measurements of external dose rate are used.

Table S4: Equivalent dose central age value and over-dispersion for each sample.

Sample	*N*	*D_e (Gy)*	*Over-dispersion (%)*	*# of components*	*Proportion of main component (%)*
UW861	312	22.8±0.4	19.3±1.6	1	100
UW1374	452	23.8±0.5	32.3±1.7	2	54.4
UW1375	398	22.5±0.4	19.8±1.7	1	100
UW1376	285	21.4±0.4	21.0±1.9	2	53.0
UW1377	401	11.7±0.3	47.8±2.3	3	53.3

Table S5: Date and information on vertical position of the OSL samples from Lapa do Santo.

Lab Id	Unit	Depth (cm)	Inferred z-value	Age (years BP)	Error
UW1376	F13	27	-0.72	11200	700
UW1375	F13	92	-1.37	12700	800
UW1374	F13	164	-2.09	12100	700
UW861	F13	132	-1.77	9900	700
UW1377	M6	214	-1.015	9500	700

Table S6: Radiocarbon dates for Lapa do Santo (table available as a .xls file)

Table S7. Chronological periods for the 2001-2009 excavations in Lapa do Santo.

	68.2% interval	95.4% interval	Vertical interval (z-value in meters)
Lapa do Santo Period 3	0.7-1.1 cal kyBP	0-2.1 cal kyBP	> 0.947
Lapa do Santo Period 2	4.0-5.2 cal kyBP	3.9-5.4 cal kyBP	0.137-0.947
Lapa do Santo Period 1	8.1-12.5 cal kyBP	8.0-12.7cal kyBP	<0.137

Table S8: Taxonomic identification of faunal remains from Lapa Santo, Number of Identified Specimens (NISP) and Minimum Number of Individuals (MNI).

Taxon	**Common name**	**NISP**	**MNI**
Amphibia	Frogs	55	5
Aves	Birds	33	4
Fish	Fishes	127	5
Mammals			
Mazama sp.	Brocket deer	137	4
Tayassu sp.	Peccaries	10	1
Carnivora	Carnivore	4	1
Dasypus novemcinctus	Nine-banded long-nose armadillo	31	4
Euphractus sexcinctus	Six-banded long-nose armadillo	6	1
Sylvilagus brasiliensis	Brazilian rabbit	4	1
Didelphidae	Common opossum	13	4
Primate	Non-human primates	3	1
Agouti paca	Paca	6	1
Rodentia	Small rodents	129	23
Reptile			
Chelonia chelidae	Turtle	6	1
	Lizards	54	4

Table S9: Skeletal representation of *Mazama* sp. at Lapa do Santo.

Skeletal Part	NISP
Calcaneus	3
Carpal	1
Tarsal	1
Horn	3
Rib	25
Innominate	2
Cranium	6
Scapula	9
Proximal phalanx	5
Medial phalanx	3
Distal phalanx	4
Femur	3
Mandible	10
Maxilla	1
Metapodial	5
Metacarpal	7
Metatarsal	26
Navicular	4
Carpal radial	1
Radius	7
Talus	10
Tibia	16
Ulna	3
Humerus	5
Cervical vertebrae	2
Thoraxic vertebrae	7
Lumbar vetebrae	1

Table S10: Correlations between skeletal abundance (%MAU) and bone density for *Mazama* sp.

SITE	***n***	***Spearman rho***	***p-value***
Guajá	90	-0.047	0.66
Gruta Cuvieri	94	0.699	<0.001
Lapa do Santo	85	0.205	0.06

Table S11: Human bone samples from Lapa do Santo. Sample analysed at: (UC) Dorothy Garrod Laboratory for Isotopic Analysis, McDonald Institute for Archaeological Research, University of Cambridge; (MPI) Isotope facilities at the Max-Planck Institute for Evolutionary Anthropology. Mean values of analyses runs given. Sample variation was <0.6‰ .

Code	$\delta^{13}C$ (‰)	$\delta^{15}N$ (‰)	C:N	Dental Development	Analysis	Runs
Burial 2	-18.9	5.2	3.1	Fully erupted	MPI	2
Burial 4	-20.3	7.7	3.5	Erupted first molar	UC	1
Burial 5	-19.5	7.2	3.2	Fully erupted	UC	3
Burial 6	-18.8	11.3	3.5	Non-erupted permanent dentition	UC	2
Burial 7	-18.2	8.8	3.1	Erupted first molar	UC	3
Burial 21	-18.8	7.0	3.2	Fully erupted	MPI	2
Burial 26	-19.0	5.9	3.0	Fully erupted	MPI	1
Burial 27	-18.8	6.5	3.1	Erupted first molar	MPI	1

Table S12: Faunal bone samples from Lagoa Santa. Sample analysed at: (UC) Dorothy Garrod Laboratory for Isotopic Analysis, McDonald Institute for Archaeological Research, University of Cambridge; (USP) Laboratório de Ecologia Isotópica, Escola Superior de Agricultura Luis de Queirós, University of São Paulo. Mean values of analyses runs given. Sample variation was <0.7‰.

Code	Site	Species	$\delta^{13}C$ (‰)	$\delta^{15}N$ (‰)	C:N	Analysis	Runs
St-3354	Lapa do Santo	*Mazama* sp.	-20.5	4.3	3.2	UC	3
St-996	Lapa do Santo	*Mazama* sp.	-21.9	4.7	3.5	UC	3
St-578	Lapa do Santo	*Euphractus sexcinctus*	-17.4	7.6	3.4	UC	3
St-743	Lapa do Santo	*Dasypus novencinctus*	-12.6	10.6	3.2	UC	3
St-548	Lapa do Santo	*Mazama* sp.	-21.2	4.6	3.2	USP	3
St-2248	Lapa do Santo	*Mazama* sp.	-21.6	5.6	3.2	USP	3
St-284	Lapa do Santo	*Dasypus novencinctus*	-14.5	9.5	3.1	USP	3
CvL2-1239	Gruta Cuvieri	*Mazama* sp.	-21.4	5.1	3.2	USP	2
CvL2-2066	Gruta Cuvieri	*Mazama* sp.	-19.1	6.9	3.2	USP	3
CvL2-3419	Gruta Cuvieri	*Mazama* sp.	-18.3	9.1	3.2	USP	1
CvL2-3419b	Gruta Cuvieri	*Mazama* sp.	-23.2	6.5	3.3	USP	1
CvL2-6333	Gruta Cuvieri	*Mazama* sp.	-18.6	9.4	3.3	USP	3
CvL2-6333b	Gruta Cuvieri	*Mazama* sp.	-21.3	4.5	3.2	USP	1
CvL2-1372	Gruta Cuvieri	Tayassuidae	-15.4	9.4	3.1	USP	2
CvL2-4443	Gruta Cuvieri	Tayassuidae	-16.7	9.7	3.2	USP	3
CvL2-2779	Gruta Cuvieri	Tayassuidae	-17.3	10.0	3.2	USP	1
CvL2-4448	Gruta Cuvieri	Tayassuidae	-22.0	5.1	3.2	USP	3
CvL2-5687	Gruta Cuvieri	Tayassuidae	-21.8	4.9	3.3	USP	2
CvL2-7185	Gruta Cuvieri	Tayassuidae	-23.6	4.2	3.3	USP	2
CvL2-7391	Gruta Cuvieri	*Dasypus novencinctus*	-16.2	10.4	3.2	USP	1
CvL2-5873	Gruta Cuvieri	*Dasypus novencinctus*	-16.2	10.7	3.2	USP	2
CvL2-5652	Gruta Cuvieri	*Euphractus sexcinctus*	-19.4	8.8	3.1	USP	3

Table S13. Contextual information of all blades found in Lapa do Santo.

Id	Raw Material	Unit	x	y	z	Period	Date of disc.
Ls-00597	?	G13	6.300	12.690	-1.013	Unkown	2002
Ls-02367	?	M05	12.305	4.868	0.756	Unkown	2002
Ls-02976	Igneous	M04	12.945	3.187	0.118	LSP2	2003
Ls-03560	Igneous	L29	11.844	28.417	-5.970	Unkown	2005
Ls-06410	Hematite	G13	6.621	12.726	-2.998	LSP1	2005
Ls-09903	Igneous	O14	14.434	13.619	-0.827	LSP1(?)	2012
Ls-11607	Igneous	P13		Surface find		Unkown	2014
Ls-11608	Igneous	Q12		Surface find		Unkown	2014

Table S14. Contextual information of all fishhooks found in Lapa do Santo.

Hook ID	Unit	Level	Raw Material	z-value	Date of recovery (dd/mm/yyyy)
1	M6	26	Bone	-0.778 to -0.968	14/07/2005
2	L23	220-230cm	Bone	-4.900 to -5.400	na/08/2005
3	L22	130-140cm	Bone	-3.700 to -4.100	na/07/2005
4	G12	22	Bone	-1.802 to -2.031	15/07/2005
5	G12	16	Bone	-1.315 to -1.425	15/07/2003
6	G12	16	Bone	-1.315 to -1.425	14/07/2003

Table S15: Blind Test Results for Heather M. Rockwell, administered December 2013.

Type of blind test	Frequency of correct identification
Location	19/20=**95%**
Relative Action	16/20=**80%**
Relative Material	18/20=**90%**
Exact Action	15.5/20=**77.5%**
Exact Material	12.5/20=**62.5%**
Total Score	**81/100=81%**

Table S16: Operation parameters for MC-ICP-MS solution analysis used at the Max-Planck Institute for Evolutionary Anthropology (Leipzig, Germany).

MC-ICP-MS	**Thermo Fisher Neptune™**
Forward power	1200 W
Reflected power	<4 W
Interface cones	Nickel
Sample cones	Nickel
Skimmer cones	Nickel (X-cone)
Coolant argon gas flow	15 L/min
Auxiliary argon gas flow	0.8 L/min
Sample gas Argon gas flow	1.17 L/min
Mass resolution	Low (400)
Lens settings	Optimized for maximum signal intensity
Nebulizer	Elemental Scientific Inc., Microflow 100µL/min, perfluoroalkoxy (PFA)
Sensitivity on ^{88}Sr	50 V/ppm
Cup configuration	L4 (^{82}Kr); L3 (^{83}Kr); L2 (^{84}Sr); L1 (^{85}Rb); Ax (^{86}Sr); H1 (^{87}Sr); H2 (^{88}Sr)
Data collection	1 block, 50 cycles, 2 s integrations

Table S17: S-EVA number, archaeological code, $^{87}Sr/^{86}Sr$ ratio, $^{84}Sr/^{86}Sr$ ratio, Sr concentration (ppm) and voltage (^{88}Sr) from enamel of the human teeth prepared in solution and analysed in the MC-ICP-MS.

S-EVA	Bur. #	Tooth	Start mass (mg)	87Sr/86Sr	$^{84}Sr/^{86}Sr$	Sr conc (ppm)	88Sr (V)
26019	Bur. 1	Inferior Right M3	23.2	0.719	0.0565	123.5	15.7
26020	Bur. 2	Superior Right P4	10.4	0.725	0.0565	181.5	15.7
26021	Bur. 3	Inferior Right P4	33.9	0.722	0.0565	41.4	17.5
26022	Bur. 4	Inferior Right dM2	21.7	0.721	0.0565	58.1	15.7
26023	Bur. 5	Superior Right M3	24	0.729	0.0565	169.9	18.4
26024	Bur. 6	Inferior Left dM2	23	0.720	0.0565	69.3	15.9
26025	Bur. 7	Inferior Left dM2	20.9	0.726	0.0565	87.3	18.1
26026	Bur. 10	Inferior Right P4	29.3	0.739	0.0564	123.3	18.0
26027	Bur. 11	Inferior Right P4	15.1	0.719	0.0565	152.9	16.4
26028	Bur. 15	Inferior Right P4	21.4	0.718	0.0564	155.4	18.2
26029	Bur. 16	Inferior Right P4	24.8	0.722	0.0565	82.8	17.1
26030	Bur. 19	Inferior Left dM2	19.7	0.717	0.0564	88.7	17.4
26031	Bur. 20	Inferior Left dM2	16	0.717	0.0565	136.7	18.2
26032	Bur. 21	Inferior Left M2	21.3	0.724	0.0564	99.7	21.3
26033	Bur. 22	Inferior Right P4	34.5	0.722	0.0564	122.6	21.2
26034	Bur. 23a	Inferior Right dM2	19.9	0.719	0.0565	65.1	21.6
26035	Bur. 23b	Inferior Right dM2	9.2	0.719	0.0565	126.5	19.4
26036	Bur. 23c	Superior Right P3	16.7	0.721	0.0564	216.5	20.1
26037	Bur. 23d	Superior Right P4	14.3	0.722	0.0565	171.4	20.5
26038	Bur. 23e	Inferior Left M2	13.4	0.720	0.0565	96.3	21.5
26039	Bur. 24	Superior Right P4	9.5	0.727	0.0565	105.8	16.8
26041	Bur. 27	Inferior Right P4	20.6	0.717	0.0565	113.5	19.6
26040	Bur. 26	Inferior Left dM2	18.9	0.724	0.0564	163.8	19.4

Table S18: Series included in the morphological affinity analyses.

Series	Region/Chronologic Affiliation	N	Reference
Lapa do Santo	Early Lagoa Santa	7	This paper
Cerca Grande	Early Lagoa Santa	5	Neves et al. 2004
Sumidouro	Early Lagoa Santa	13	Neves et al. 2007b
Early Colombia	Early Colombia	38	Neves et al. 2007a
Archaic Colombia	Archaic Colombia	14	Neves et al. 2007a
Peru	South America	110	Howells 1973, 1989
Arikara	North America	69	Howells 1973, 1989
Santa Cruz	North America	102	Howells 1973, 1989
Buriat	NE Asia	109	Howells 1973, 1989
Anyang	East Asia	42	Howells 1973, 1989
Atayal	East Asia	47	Howells 1973, 1989
Hainan	East Asia	83	Howells 1973, 1989
Northern Japan	East Asia	87	Howells 1973, 1989
Southern Japan	East Asia	91	Howells 1973, 1989
Australia	Australo-Melanesia	101	Howells 1973, 1989
Tasmania	Australo-Melanesia	87	Howells 1973, 1989
Tolai	Australo-Melanesia	110	Howells 1973, 1989
Berg	Europe	109	Howells 1973, 1989
Norse	Europe	110	Howells 1973, 1989
Zalavar	Europe	98	Howells 1973, 1989
Bushman	Sub-saharan Africa	90	Howells 1973, 1989
Dogon	Sub-saharan Africa	99	Howells 1973, 1989
Teita	Sub-saharan Africa	83	Howells 1973, 1989
Zulu	Sub-saharan Africa	101	Howells 1973, 1989
Easter Island	Polynesia	86	Howells 1973, 1989

Table S19: Craniometric measurements used in the morphological affinity analyses.

Glabello-occipital length (GOL)	Nasion Subtense (NAS)
Nasio-occipital length (NOL)	Interorbital breadth (DKB)
Maximum cranial breadth (XCB)	Cheek height (WMH)
Maximum frontal breadth (XFB)	Supraorbital substense (SOS)
Nasion-prosthion height (NPH)	Glabella subtense (GLS)
Nasal height (NLH)	Frontal cord (FRC)
Orbit height (OBH)	Frontal subtense (FRS)
Orbit breadth (OBB)	Frontal fraction (FRF)
Mastoid Height (MDH)	Parietal cord (PAC)
Mastoid Breadth (MDB)	Parietal subtense (PAS)
Bifrontomallare breadth (FMB)	Parietal fraction (PAF)

Table S20: Estimation of sex and age at death for the skeletons of Lapa do Santo (table available as a .xls file).

14. Expanded reference list[1]

ACEITUNO, F.J., N. LOAIZA, M.E. DELGADO-BURBANO. & G. BARRIENTOS. 2013. The initial human settlement of Northwest South America during the Pleistocene/Holocene transition: synthesis and perspectives *Quaternary International* 301: 23–33.

ARAUJO, A.G.M. 2010. *Lapa das Boleiras - Um sítio paleoíndio do carste de Lagoa Santa, MG, Brazil*. São Paulo: Annablume.

ARAUJO, A.G.M., J.K. FEATHERS., M. ARROYO-KALIN & M.M. TIZUKA. 2008. Lapa das Boleiras rockshelter: stratigraphy and formation processes at a paleoamerican site in Central Brazil *Journal of Archaeological Science* 35: 3186–202.

ARAUJO, A.G.M., W.A. NEVES & R. KIPNIS. 2012. Lagoa Santa revisited: an overview of the chronology, subsistence, and material culture of paleoindian sites in eastern central Brazil *Latin American Antiquity* 23: 533–50.

ARAUJO, A.G.M., W.A. NEVES, L.B. PILÓ & J.P.V. ATUI. 2005. Holocene dryness and human occupation in Brazil during the 'Archaic Gap' *Quaternary Research* 64: 298–307.

ARRIAZA, B. 1995. Chinchorro bioarchaeology: chronology and mummy seriation *American Antiquity* 6: 35–55.

BÁNYAI, M. 1997. *Minhas pesquisas arqueológicas na região de Lagoa Santa*. Symbiose.

BERNARDO, D.V., A.M. STRAUSS, W.A. NEVES & M. OKUMURA. 2011. Measuring skulls, getting into the biological realm of the settlement of the New World, in D. Vialou (ed.) *Peuplements et préhistoire en Amériques*: 31–41. Paris: Éditions du Comité des travaux historiques et scientifiques.

BINFORD, L.R. 1971. Mortuary practices: their study and their potential *Memoirs of the Society for American Archaeology*: 6–29.

BOËDA, E., I. CLEMENTE-CONTE, M. FONTUGNE, C. LAHAYE, M. PINO, G.D. FELICE, N. GUIDON, S. HOELTZ, A. LOURDEAU, M. PAGLI, A.-M. PESSIS, S. VIANA, A. DA COSTA & E. DOUVILLE. 2014. A new late Pleistocene archaeological sequence in South America: the Vale da Pedra Furada (Piauí, Brazil) *Antiquity* 88: 927–41.

BOËDA, E., A. LOURDEAU, C. LAHAYE, G.D. FELICE, S. VIANA, I. CLEMENTE-CONTE, M. PINO, M. FONTUGNE, S. HOELTZ, N. GUIDON, A.-M. PESSIS, A. DA-COSTA & M. PAGLI. 2013. The late Pleistocene industrie of Piauí, Brazil: new data, in K. Graf, C.

[1] Expanded reference list including relevant works not cited in the main text.

Ketron & M. Water (ed.) *Paleoamerican Odyssey*: 445–65. Austin.

BORRERO, L.A. 2015. Moving: hunter-gatherers and the cultural geography of South America *Quaternary International* 363: 126–33.

BROWN, J. 2010. Cosmological layouts of secondary burial as political instrument, in L. Sullivan & M. RC (ed.) *Mississippian mortuary practices - beyond hierarchy and the representationist perspective*, 1st ed. Florida: University Press of Florida.

BUENO, L., A.S. DIAS & J. STEELE. 2013. The Late Pleistocene/Early Holocene archaeological record in Brazil: a geo-referenced database *Quaternary International* 301. Elsevier: 74–93.

CANNON, A., B. BARTEL, R. BRADLEY, R.. CHAPMAN, M. Lou CURRAN, D.W.J. GILL, S.C. HUMPHREYS, C. MASSET, I. MORRIS, J. QUILTER, A. NAN & C. RUNNELS. 1989. The historical dimension in mortuary expressions of status and sentiment *Current Anthropology* 30: 437–58.

CAPRILES, J.M. & J. ALBARRACIN-JORDAN. 2013. The earliest human occupations in Bolivia: a review of the archaeological evidence *Quaternary International* 301: 46–59.

CARDICH, A. 1964. *Lauricocha - fundamentos para uma prehistoria de los Andes Centrales*. Buenos Aires.

CARR, C. 1995. Mortuary practices: their social, philosophical-religious, circumstantial, and physical determinants *Journal of Archaeological Method and Theory* 2: 105–200.

CARTELLE, C. 1994. *Tempo passado: mamíferos fósseis em Minas Gerais*. Belo Horizonte: Editora Palco.

CHAPMAN, R. 2005. Mortuary analysis: a matter of time, in G. Rakita, J. Buikstra, L. Beck & S. Williams (ed.) *Interacting with the dead – Perspectives on mortuary archaeology for the New Millennium1*: 25–40. Florida: University Press of Florida.

CHARLES, D.K. & J. BUIKSTRA. 1983. Archaic mortuary sites in the central Mississippi drainage: distribution, structure and behavioral implications, in J. Phillips & J. Brown (ed.) *Archaic hunters and gatherers in the American midwest.* New York: Academic Press.

CHAUCHAT, C. & J.P. LA COMBE. 1984. El hombre de Paijan: el mas antiguo peruano? *Gaceta Arqueologica Andina* 11: 4–6.

CHESSON, M.S. 1999. Libraries of the dead: early bronze age charnel houses and social identity at urban Bab edh-Dhra', Jordan *Journal of Anthropological Archaeology* 18: 137–64.

CORDY-COLLINS, A. 1992. Archaism or tradition? The decapitation theme in

Cupisnique and Moche iconography *Latin American Antiquity* 3: 206–20.
CORREAL, G. 1990. *Aguazuque evidencias de cazadores, recolectores y plantadores em la altiplanice de la cordillera oriental*. Bogotá: Fundación de Investigaciones Arqueológicas Nacionales.
COSTA-JUNQUEIRA, M.A. 2001. Modalidades de enterramientos humanos arcaicos em el Norte de Chile *Revista Chungará* 33: 55–62.
DA-GLORIA, P. 2012. Health and lifestyle in the Paleoamericans: early Holocene biocultural adaptation at Lagoa Santa, central Brazil. The Ohio State University.
DA-GLORIA, P., A.M. STRAUSS & W.A. NEVES. 2011. Mortuary rituals in the Early Holocene population of Lagoa Santa: the Harold Walter collection *American Journal of Physical Anthropology* 144: 119.
DEETZ, J. & E.N. DETHLEFSEN. 1971. Some social aspects of New England colonial mortuary art, in J. Brown (ed.) *Memoir of the Society for American Archaeology*: 30–38.
DILLEHAY, T.D. 1997. ¿Donde estan los restos oseos humanos del periodo Pleistocene tardio? *Boletin de Arqueologia PUCP* 1: 55–63.
DILLEHAY, T.D., C. OCAMPO, J. SAAVEDRA, A.O. SAWAKUCHI, R.M. VEGA, M. PINO, M.B. COLLINS, L.S. CUMMINGS, I. ARREGUI, X.S. VILLAGRAN, G.A. HARTMANN, M. MELLA, A. GONZÁLEZ & G. DIX. 2015. New archaeological evidence for an early human presence at Monte Verde, Chile *PLoS ONE* 10: 1–28.
EGGERS, S., M. PARKS, G. GRUPE & K.J. REINHARD. 2011. Paleoamerican diet, migration and morphology in Brazil: archaeological complexity of the earliest Americans. *PloS one* 6: e23962.
FEHREN-SCHMITZ, L., B. LLAMAS, S. LINDAUER, E. TOMASTO-CAGIGAO, S. KUZMINSKY, N. ROHLAND, F.R. SANTOS, P. KAULICKE, G. VALVERDE, S.M. RICHARDS, S. NORDENFELT, V. SEIDENBERG, S. MALLICK, A. COOPER, D. REICH & W. HAAK. 2015. A re-appraisal of the early Andean human remains from Lauricocha in Peru *PLoS ONE* 10: 1–13.
FERGUSON, R.B. 1990. Blood of the Leviathan: western contact and warfare in Amazonia *American Ethnologist* 17: 237–57.
GOLDSTEIN, L.G. 1976. Spatial structure and social organization: regional manifestations of Missesissippian. Northwestern University.
– 2000. *Mississippian ritual secondary disposal*. (ed.) S.R. Ahler *Mounds, Modoc, and Mesoamerica: papers in honor of Melvin L. Fowler.* Springfield: Illinois State Museum

Scientific Papers.

HANSEN, S. 1888. *En Anthropologisk Undersogelse af Jordfundne Menneskelevninger fra Brasilianske Huler. Med et Tillaeg om det Jordfundne Menneske fra Pontimelo*. La Plata: Rio de Arrecifes.

HERTZ, R. 1907. Contribuition à une étude sur la représentation collective de la mort *Année sociologique* 10: 48–137.

HRDLÍČKA, A. 1912. Early Man in South America *Bureau of American Ethnology* 52.

HUNTINGTON, R. & P. METCALF. 1979. *Celebrations of death: the anthropology of mortuary ritual*. Cambridge: Cambridge University Press.

HURT, W. & O. BLASI. 1969. O Projeto Arqueológico Lagoa Santa – Minas Gerais, Brasil (nota final) *Arquivos do Museu Paranaense* 4: 1–63.

KALTWASSER, J., A. MEDINA & J. MUNIZAGA. 1986. El hombre de Cuchipuy. Prehistoria de Chile central en el Período Arcaico. *Revista Chungará* 16-17: 99–105.

KIPNIS, R. 1998. Early hunter-gatherers in the Americas: perspectives from Central Brazil *Antiquity* 72: 581–92.

– 2002. Foraging societies of eastern central Brazil: an evolutionary ecology study of subsistence strategies during the terminal Pleistocene and early/middle Holocene. University of Michigan.

KOKABI, M., G. AMBERGER & J. WAHL. 1994. Die knochenfunde aus der Villa rustica von Bondorf *Die Villa rustica von Bondorf* 51: 285–335.

KOLLMAN, J. 1884. Schadeln von Lagoa Santa *Z. Ethnology* 16: 194–99.

KROEBER, A. 1927. Disposal of the dead *American Anthropologist* 29: 308–15.

KUIJT, I. 1996. Negotiating equality through ritual: a consideration of Late Natufian and Prepottery Neolithic A period mortuary practices *Journal of Anthropological Archaeology* 15: 313–36.

LAHAYE, C., M. HERNANDEZ, E. BOËDA, G.D. FELICE, N. GUIDON, S. HOELTZ, A. LOURDEAU, M. PAGLI, A.-M. PESSIS, M. RASSE & S. VIANA. 2013. Human occupation in South America by 20,000 BC: the Toca da Tira Peia site, Piauí, Brazil *Journal of Archaeological Science* 40: 2840–47.

LAMING-EMPERAIRE, A. 1979. Missions archéologiques franco-brésiliennes de Lagoa Santa, Minas Gerais, Brésil – Le Grand abri de Lapa Vermelha *Revista de Pré-história* 1: 53–89.

LAVALLÉE, D. 1995. *The first South Americans - the peopling of a continent from the earliest evidence to high culture*. Salt Lake City: The University of Utah Press.

LITTLETON, J. & H. ALLEN. 2007. Hunter-gatherer burials and the creation of persistent places in southeastern Australia *Journal of Anthropological Archaeology* 26: 283–98.
LLAGOSTERA, A. 2003. Patrones de momificación Chinchorro en las colecciones Uhle y Nielsen *Chungara* 35: 5–22.
LUNA, P. 2007. Peter Wilhelm Lund: o auge das suas investigações científicas e a razão para o término das suas pesquisas. Universidade São Paulo.
LUND, P.W. 1844. Notícia sobre ossadas humanas fósseis achadas numa caverna do Brasil, in P. Couto (ed.) *Memórias sobre a paleontologia brasileira*. Rio de Janeiro: Instituto Nacional do Livro.
MARTÍNEZ, G., G. FLENSBORG & P.D. BAYALA. 2013. Chronology and human settlement in northeastern Patagonia (Argentina): patterns of site destruction, intensity of archaeological signal, and population dynamics *Quaternary International2* 301: 123–34.
MAYBURY-LEWIS, D. 1979. *Dialectical societies: the Gê and Bororo of central Brazil*. Harvard: Harvard University Press.
MAZZ, J.L. 2013. Early human occupation or Uruguay: radiocarbon database and archaeological implications *Quaternary International* 301: 94–103.
MELGAR, C.M. 2013. Terminal Pleistocene/early Holocene 14C dates from archaeological sites in Chile: critical chronological issues for the initial peopling of the region *Quaternary International* 301: 60–73.
MENA, F.L., O.B. REYES, T.W. STAFFORD & J. SOUTHON. 2003. Early human remains from Ba??o Nuevo-1 cave, central Patagonian Andes, Chile *Quaternary International* 109-110: 113–21.
MESSIAS, T. & M.C. MELLO E ALVIM. 1961. Material das escavações arqueológicas na região de Lagoa Santa, Minas Gerais, Brasil (1956) *Boletim do Museu Nacional N.S. Antropologia* 20: 1–55.
METCALF, P. 1981. Meaning and materialism: the ritual economy of death. *Man* 16: 563–78.
NELSON, A.R. 2005. 'Osteobiographics' of dos Coqueiros reconsidered: Comment on Lessa and Guidon (2002) *American Journal of Physical Anthropology* 126.
NEVES, W.A., A.G.M. ARAUJO, D.V. BERNARDO, R. KIPNIS & J.K. FEATHERS. 2012. Rock art at the Pleistocene/Holocene boundary in eastern South America. *PloS one* 7: e32228.
NEVES, W.A., R. GONZÁLEZ-JOSÉ, M. HUBBE, R. KIPNIS, A.G.M. ARAUJO & O. BLASI.

2004. Early Holocene human skeletal remains from Cerca Grande, Lagoa Santa, Central Brazil, and the origins of the first Americans *World Archaeology* 36: 479–501.

NEVES, W.A. & M. HUBBE. 2005. Cranial morphology of early Americans from Lagoa Santa, Brazil: implications for the settlement of the New World. *Proceedings of the National Academy of Sciences of the United States of America* 102: 18309–14.

NEVES, W.A., M. HUBBE, D. BERNARDO, A.M. STRAUSS, A.G.M. ARAUJO & R. KIPNIS. 2013. Early human occupation of Lagoa Santa, Eastern Central Brazil: craniometric variation of the initial settlers of South America, in K. Graf, C. Ketron & M. Water (ed.) *Paleoamerican odyssey*: 397–412. Texas A&M University Press.

NEVES, W.A., M. HUBBE & G. CORREAL. 2007. Human skeletal remains from Sabana de Bogota Colombia : a case of Paleoamerican morphology late survival in South America ? *American Journal of Physical Anthropology* 133: 1080–98.

NEVES, W.A., A. PROUS, R. GONZALEZ JOSE, R. KIPNIS & J. POWELL. 2003. Early Holocene human skeletal remains from Santana do Riacho, Brazil: implications for the settlement of the New World *Journal of Human Evolution* 45: 19–42.

O'SHEA, J. 1984. *Mortuary variability: an archaeological investigation*. New York: Academic Press.

OKUMURA, M. & A.G.M. ARAUJO. 2014. Long-term cultural stability in hunter–gatherers: a case study using traditional and geometric morphometric analysis of lithic stemmed bifacial points from Southern Brazil *Journal of Archaeological Science* 45. Elsevier Ltd: 59–71.

PARDOE, C. 1988. Cemetery as symbol. The distribution of prehistoric aboriginal grounds in southeastern Australia *Archaeology in Oceania* 16: 173–78.

PESSIS, A.-M. 2013. *Images from pre-history*. São Paulo: FUMDHAM.

PILÓ, L.B. & A.S. AULER. 2002. Apresentação: bicentenário de Peter Wilhelm Lund (1801-1880) *O Carste* 14: 4–7.

PRATES, L., G. POLITIS & J. STEELE. 2013. Radiocarbon chronology of the early human occupation of Argentina *Quaternary International* 301: 104–22.

PROUS, A. 1992. As estruturas aparentes: os sepultamentos do Grande Abrigo de Santana do Riacho. Os sepultamentos da escavação N°1 *Arquivos do Museu de História Natural*.

PROUS, A. & M.C. SCHLOBACH. 1997. Sepultamentos pré-históricos do Vale do Peruaçu - MG. *Revista do Museu de Arqueologia e Etnologia da Universidade de São Paulo* 7: 3–21.

PUCCIARELLI, H.M., S.I. PEREZ & G.G. POLITIS. 2010. Early Holocene human remains from the Argentinean Pampas: additional evidence for distinctive cranial morphology of early South Americans. *American Journal of Physical Anthropology* 143: 298–305.

PUGLIESE, F. 2008. Os líticos de Lagoa Santa: um estudo sobre organização tecnológica de caçadores-coletores do Brasil Central. Universidade de São Paulo.

QUILTER, J. 1989. *Life and death at Paloma - Society and mortuary practices in a preceramic Peruvian village.* Iowa: University of Iowa Press.

RADEMAKER, K., G.R.M. BROMLEY & D.H. SANDWEISS. 2013. Peru archaeological radiocarbon database, 13,000-7000 14C B.P. *Quaternary International* 301: 34–45.

RAKITA, G. & J. BUIKSTRA. 2005. Corrupting flesh: reexamining Hertz's perspective on mummification, in G. Rakita, J. Buikstra, L. Beck & S. Williams (ed.) *Interacting with the dead – perspectives on mortuary archaeology for the New Millennium*. Florida: University Press of Florida.

ROSSEN, J. & T.D. DILLEHAY. 2001. Bone cutting, placement, and cannibalism? Middle preceramic mortuary patterns of Nanchoc, northern Peru *Chungara* 33: 63–72.

ROSTWOROWSKI, M. 1983. *Estructuras andinas del poder. Ideologia religiosa y política.* Lima: Instituto de Estudios Peruanos.

SANTORO, C.M., V.G. STANDEN, B.T. ARRIAZA & T.D. DILLEHAY. 2005. Archaic funerary pattern or postdepositional alteration? The Patapatane Burial in the Highlands of South Central Andes. *Latin American Antiquity* 16: 329–46.

SAXE, A. 1970. *Social dimensions of mortuary practices*. University of Michigan.

SAXE, A. & P.L. GALL. 1977. Ecological determinants of mortuary practices: the Temuan of Malysia, in *Cultural-ecological perspectives on Southeast Asia.*

SCHEINSOHN, V. 2003. Hunter-gatherer archaeology in South America *Annual Review of Anthropology* 32: 339–61.

SCHLANGER, S.H. 1992. Recognizing persistent places in Anasazi settlement systems, in J. Rossignol & L. Wandsnider (ed.) *Space, time, and archaeological landscapes*: 91–112. New York: Plenum Press.

SCHROEDER, S. 2001. Secondary disposal of the dead: cross-cultural codes. *World Cultures* 12: 77–93.

SOFAER, J.R. 2006. *The body as material culture - a theoretical osteoarchaeology*. Cambridge: Cambridge University Press.

SOUZA, R. 2011. As tecnologias esqueletais: uma investigação sobre o uso de matérias-primas de origem esqueletal por meio de análise comparativa entre coleções

arqueológicas e etnográficas. Universidade de São Paulo.

STOTHERT, K. 1985. The preceramic Las Vegas culture of Coastal Ecuador *American Antiquity* 50: 613–37.

STRAUSS, A.M., M. HUBBE, W.A. NEVES, D. V BERNARDO & J.P.V. ATUI. 2015. The cranial morphology of the Botocudo Indians, Brazil. *American Journal of Physical Anthropology* 157:202-216.

STRAUSS, A.M., E. KOOLE, R.E. De OLIVEIRA, M. INGLEZ, T. NUNES, P. DA-GLORIA, F. COSTA & W.A. NEVES. 2011. Two directly dated Early-Holocene Archaic burials from Pains, State of Minas Gerais, Brazil. *Current Research on Pleistocene* 28: 123–25.

TAINTER, J.A. 1978. Mortuary practices and the study of prehistoric social systems. *Advances in Archaeological Method and Theory* 1: 105–41.

TEN KATE, H. 1885. Sur les Crânes de Lagoa Santa *Bulletin of Social Anthropology* 8: 240–44.

UCKO, P.J. 1969. Ethnography and archaeological interpretation of funerary remains. *World Archaeology* 1: 262–80.

VERANO, J.W., S. UCEDA, C. CHAPDELAINE, R. TELLO, M. ISABEL, V. PIMENTEL & M.I. PAREDES. 1999. Modified human skulls from the urban sector of the pyramids of Moche, northern Peru. *Latin American Antiquity* 10: 59–70.

VERGNE, C. 2002. Estruturas funerárias do sítio Justino: distribuição no espaço e no tempo. *Canindé* 2: 251–73.

VILLAGRAN, X., A.M. STRAUSS, C. MILLER., B. LIGOUIS & R. OLIVEIRA. *In press*. Buried in the ashes: formation processes of an early South American's site (Lapa do Santo, Brazil). *Journal of Archaeological Science*.

VIVEIROS DE CASTRO, E. 1992. *From the enemy's point of view - humanity and divinity in an Amazonian Society*. Chicago: University of Chicago Press.

WAHL, J. 1994. Manipuliert menschenknochen aus Baden-Württemberg. *Archäologische Information aus Baden-Württemberg* 27: 129–40.

WALTER, H.V. 1958. *Arqueologia da região de Lagoa Santa. SEDEGRA, Rio de Janeiro*. Rio de Janeiro: SEDEGRA.

WALTER, H. V., A. CATHOUD & A. MATTOS. 1937. The Confins Man. A contribution to the study of Early Man in South America, in G.G. MacCurdy (ed.) *Early Man – as depicted by leading authorities at the international symposium the Academy of Natural Sciences Phyladelphia*. London: J. B. Lippincott Company.

WALTHALL, J.A. 1999. Mortuary behavior and Early Holocene land use in the North

American midcontinent. *North American Archaeologist* 20: 1–30.

15. Detailed legends for figures in the main text

Figure 1. Left: map of showing the Lagoa Santa region (red star) and other sites mentioned in the text: Baño Nuevo (yellow diamond), Huchichocana Cave (black diamond), La Chimba (purple diamond), La Fundición (orange diamond), Lauricocha (light blue diamond), Pampa de los Fóssiles (light green diamond), Tequendama (white diamond), Capelinha (black square), Justino (green square), Loca do Suim (yellow square), Santana do Riacho (white square) and Toca dos Coqueiros (blue square). Right: Aerial view of the Lapa do Santo massif. The black arrow indicates the archaeological site.

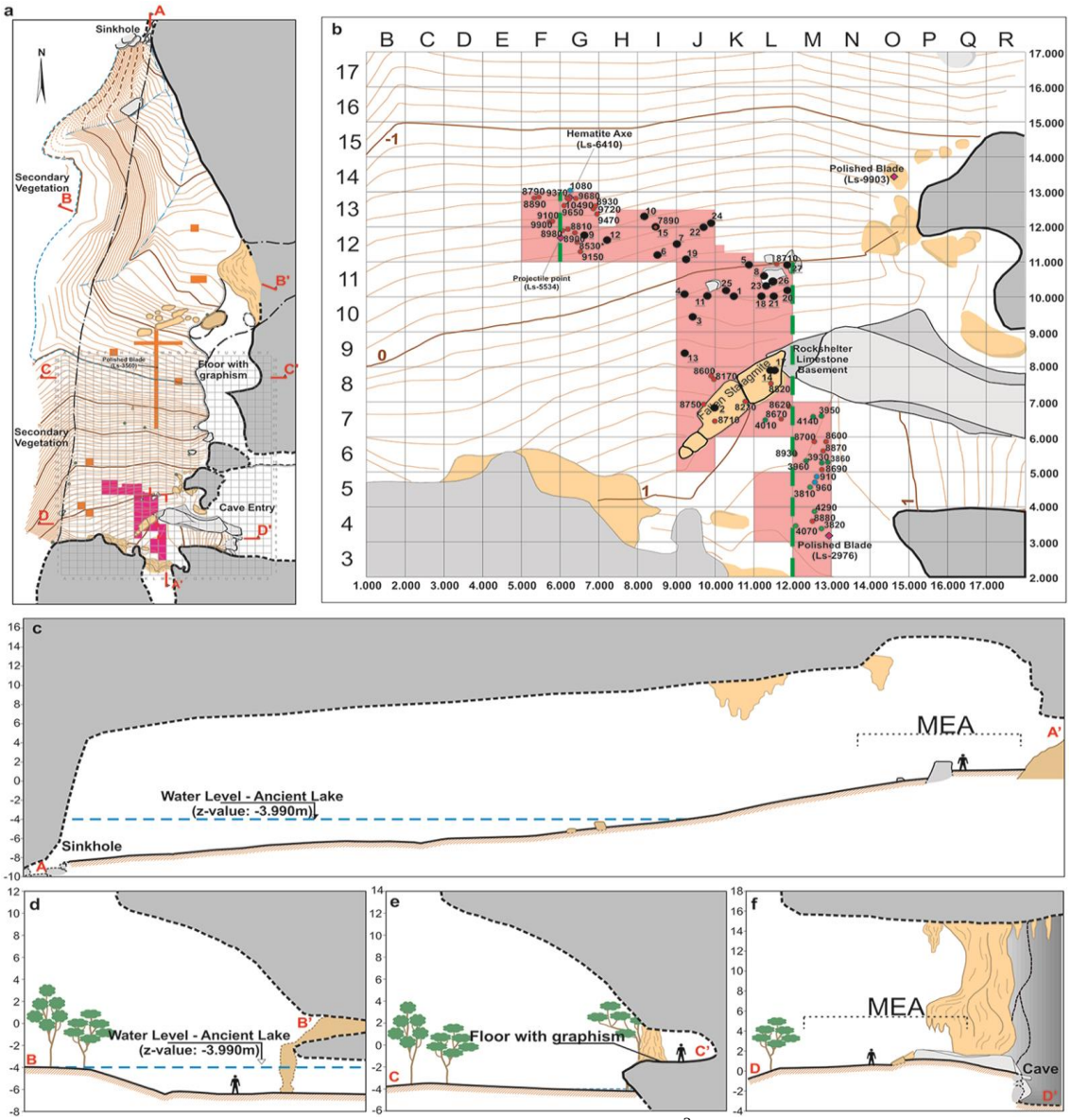

Figure 2. a) plan of Lapa do Santo. The grid corresponds to 1 m^2. Pink and orange indicate excavated surfaces. Pink indicates the main excavation area (MEA); bedrock is grey and secondary deposits (eg breccia and stalagmites) in beige. The topographic lines are 10 cm equidistant and the associated values correspond to the z-value of the site coordinate system. The red letters indicate the start and end of the sections depicted below; b) detail of the MEA. Red, green and blue dots are, respectively, early, middle and late Holocene charcoal samples with the radiocarbon non-calibrated dates. Black disks indicate human burials. Numbers in the margins indicate x and y values from the coordinate system of site. The dashed green lines indicate the surfaces of the profiles in Figure S3; c) profile from points A to A'; d) section from points B to B' e) section from points C to C'; f) section from points D to D'.

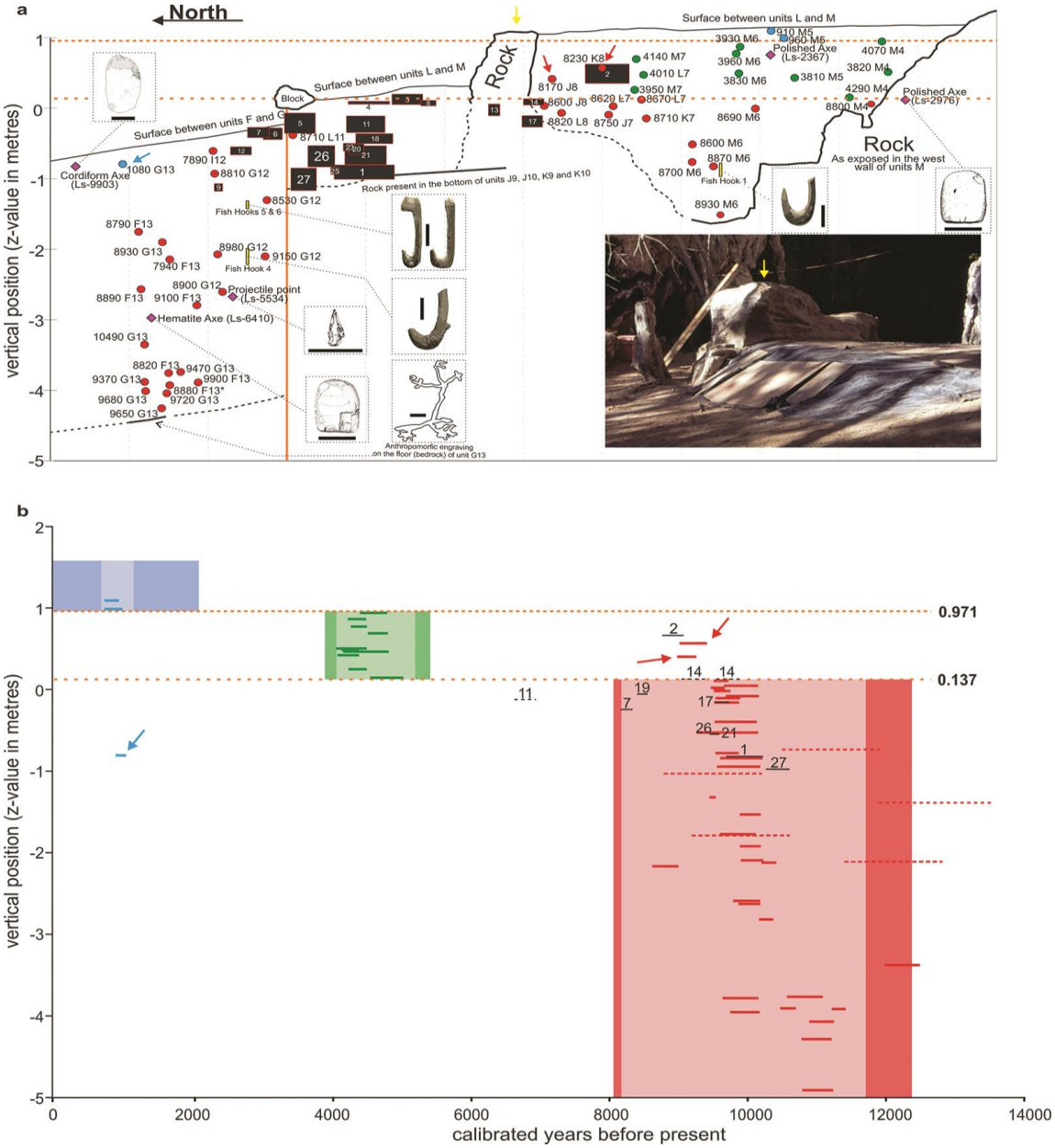

Figure 3a. Chronology of Lapa do Santo: a) South-North section following the surfaces indicated with the dashed green line in the Figure S1. The continuous thin black line indicates the original surface of the archaeological deposit before excavations. The continuous and pointed thick black line indicates observed and inferred rockshelter's floor and walls, respectively. Red, green and blue dots are dated charcoal belonging to Lapa do Santo Period (LSP) 1, 2 and 3, respectively. The number next to the dots indicates the radiocarbon non-calibrated age and the unit where the charcoal was located. The numbers in the left frame indicate the z-values in meters. Black rectangles show the position and dimensions of the burials and their respective identification is indicated by the white number. The picture in the detail was taken from a similar angle as the one of the profile and the yellow arrows point to the rock that is also represented in the schematic profile. Note the presence of a steep transition in the surface of the site between the south (right side from the rock in the picture) and the north (left side of rock in the picture) regions. This is exactly where the fallen stalagmite was located, which was removed for excavation under it. See legend of "b" for meaning of the blue and red arrows and also for dashed and dotted orange lines.

Figure 3b. Chronology of Lapa do Santo: b) Scatterplot showing the relationship between vertical position (z-value) and age for different components of Lapa do Santo. Red, green and blue horizontal continuous bars indicated the 95.4%interval of the modelled calibrated radiocarbon dates obtained from charcoal samples. Black and dashed horizontal continuous bars indicate the 95.4%interval of the modelled and non-modelled calibrated radiocarbon dates obtained from bone collagen, respectively. The associated number indicates the burial accession number. Red horizontal dashed bars indicate the 95.4% interval of the OSL dates. The blue, green and red zones indicate the 68.2% (light color) and 95.4% intervals (strong color) of LSP-1, LSP-2 and LSP-3 (see Supplementary Information for details). The orange dotted and dashed lines indicate, respectively, the average z-value that set apart LSP-3 from LSP-2 and LSP-2 from LSP-1. The blue and red arrows point to the three charcoals that present z-values incompatible with the boundaries defined between LSPs. They are correspondent to the arrows in "b". Note that Burial 11 does not belong to any of the defined periods.

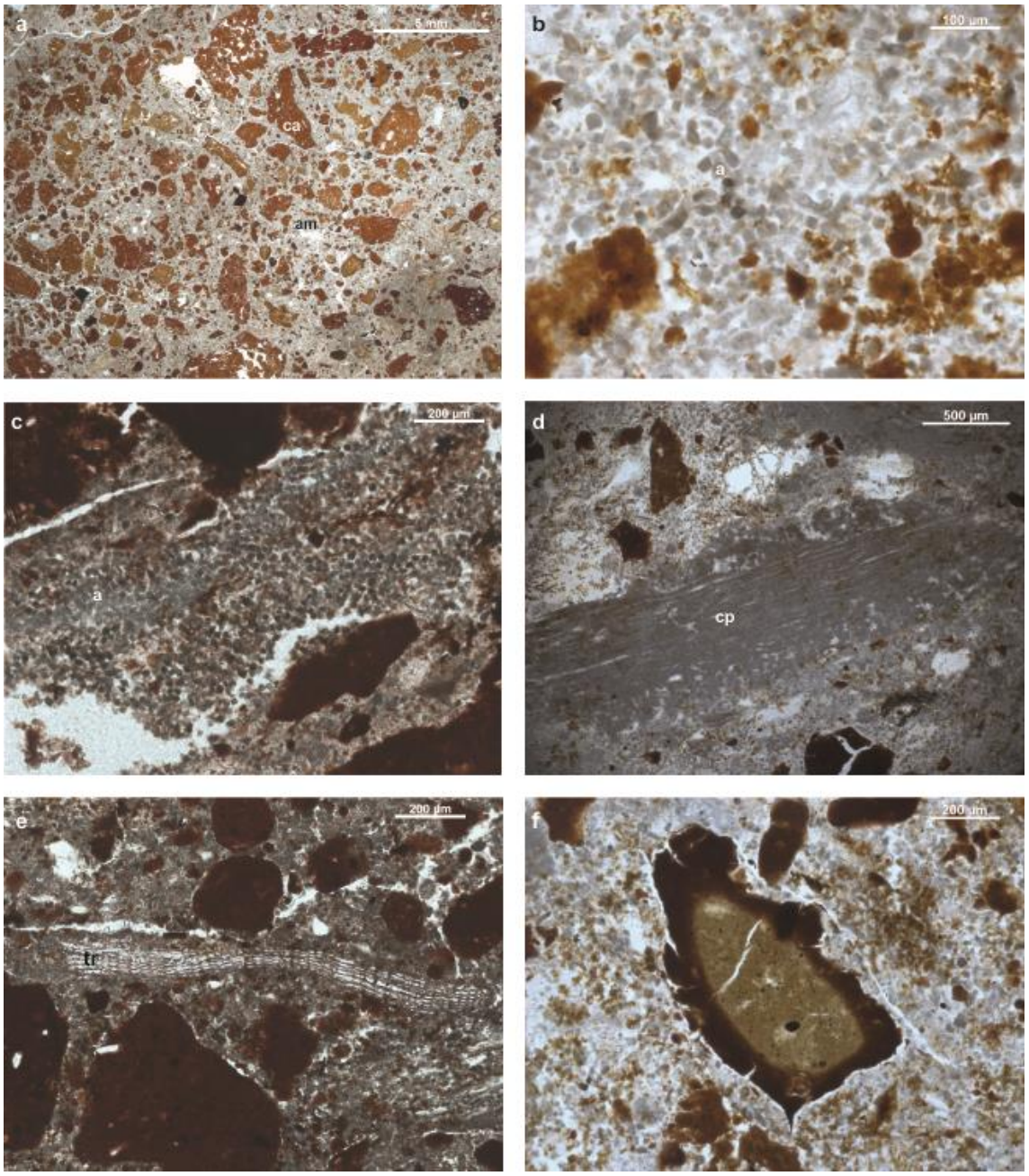

Figure 4. Photomicrographs of thin sections from Lapa do Santo. a) groundmass made of clay aggregates (ca) in micromass consisting of plant ashes. b, well-preserved ash crystals (a). c, layer of ash crystals in-between red clay aggregates. d, charcoal pseudo-morph (cp) made of arranged ash crystals that maintain the cell structure of the charcoal. e, silicified tissue residue (tr). f, yellow clay aggregate with dark red rim suggesting burning.

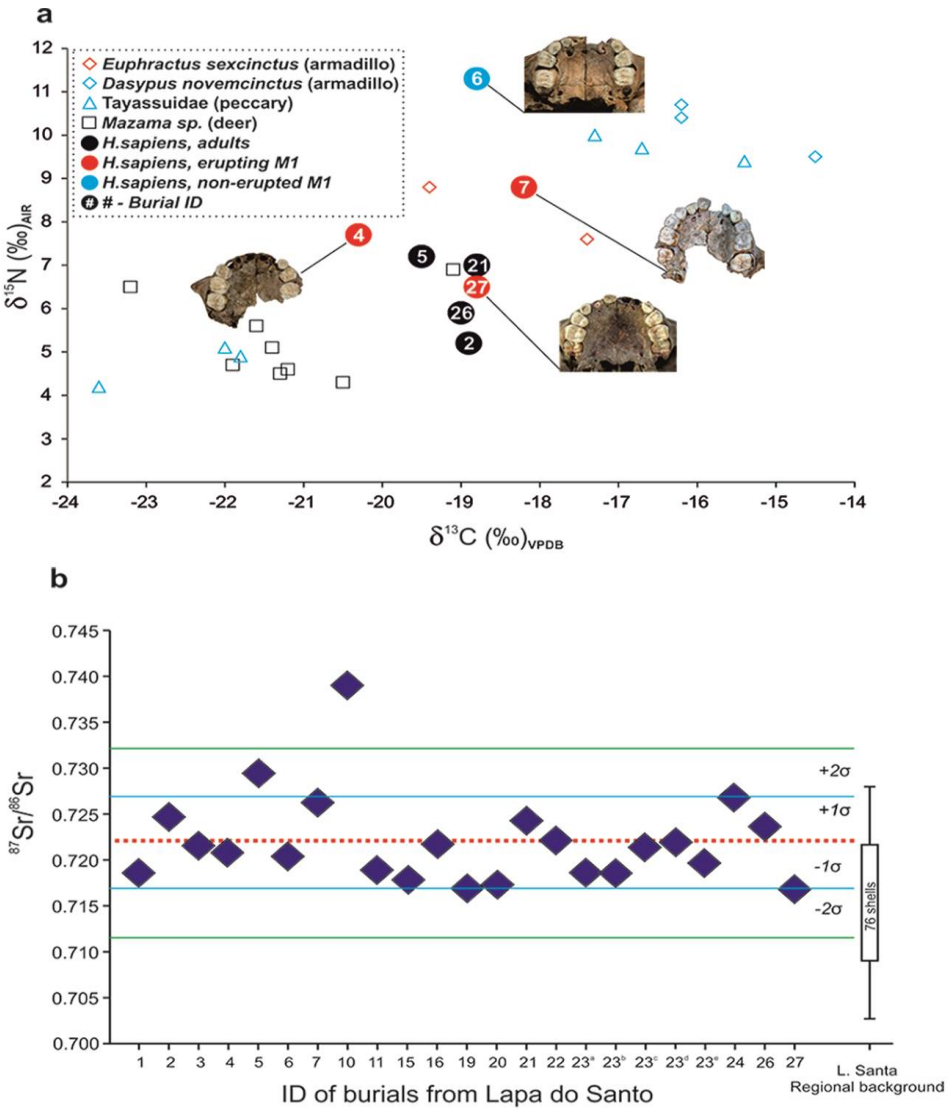

Figure 5. Isotopes analyses. a, $\delta^{15}N$ and $\delta^{13}C$ values of bone collagen from humans and animals from Lagoa Santa region. Black squares: *Mazama sp.* (deer); blue triangles: Tayassuidae (peccary); blue diamonds: *Dasypus novemcinctus* (nine-banded armadillo); red diamonds: *Euphractus sexcinctus* (six-banded armadillo); black disks: adult humans with fully occluded permanente dentition; red disks: sub-adult humans with erupted permament first molar; blue disk: sub-adult human with non-erupted permanent dentition. The number inside the black disks indicates the identification number of the burial. Maxilla photos depict dental development stage for the non-adult individuals. b, Enamel $^{87}Sr/^{86}Sr$ ratio values from the individuals of Lapa do Santo, plotted on $^{87}Sr/^{86}Sr$ mean ratio value (red dashed line), mean ratio ± 1σ values (area between blue lines), and mean ratio ± 2σ values (area between green lines) of the entire human population. The box plot indicates the descriptive statistics (mean, standard deviation and two standard deviations) for the 76 sampled of shells characterizing Lagoa Santa strontium bioavailability.

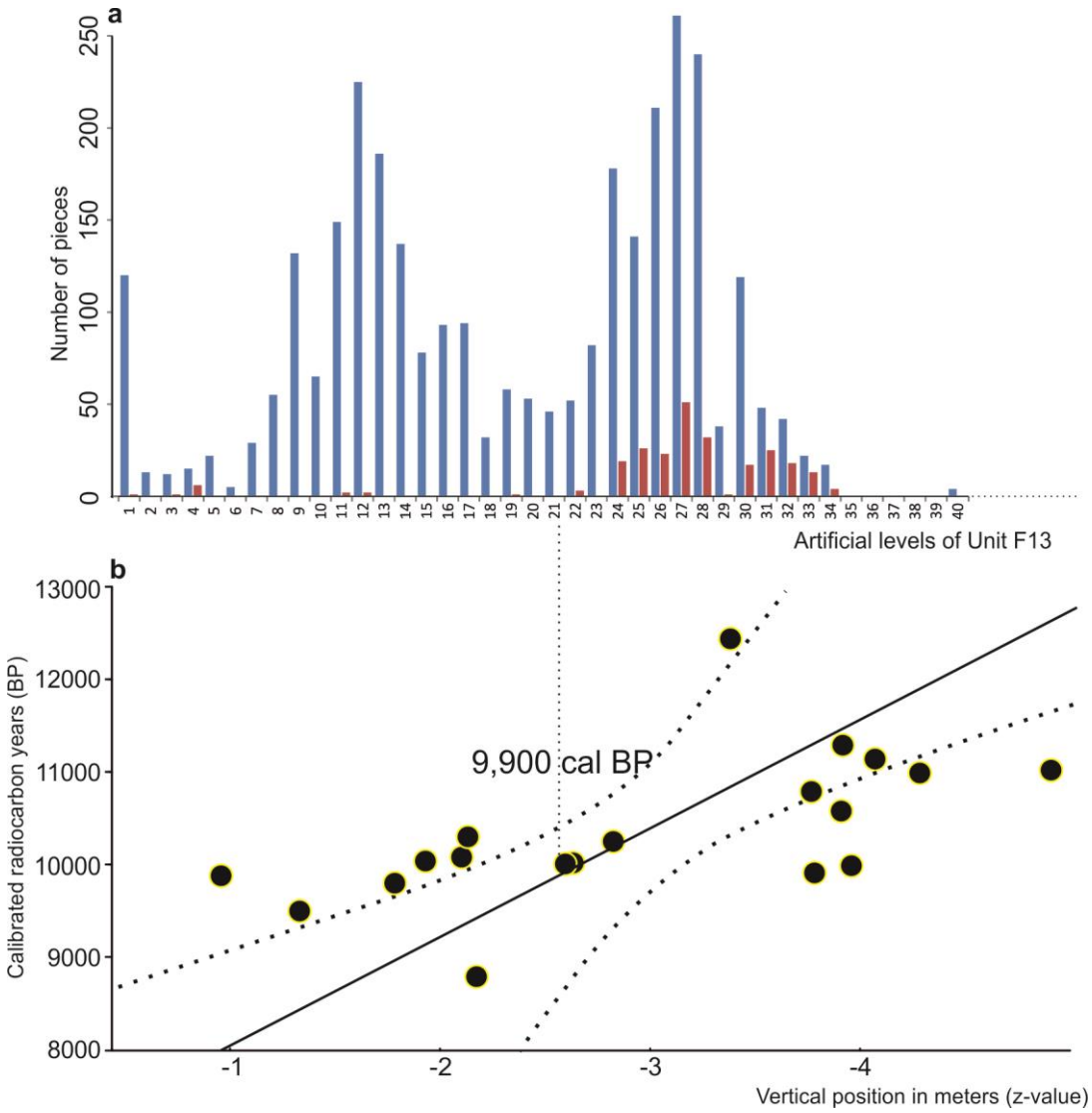

Figure 6. Chronological behavior of lithic abundance and type of raw material in Lapa do Santo during early Holocene. a, Histogram of quartz (blue bars) and silexite (red bars) abundance along Lapa do Santo`s unit F13 stratigraphy. Note that after level 22 silexite, which is an allochthonous raw material, is no longer used in the site. b, The event identified in the histogram are dated by comparing its vertical position (z-value) with the calibrated radiocarbon dates from charcoals (black disks) from unit F13 and the adjacent unit G13 in correspondent vertical position. The x-axis of both graphs are in aligned and in the same scale.

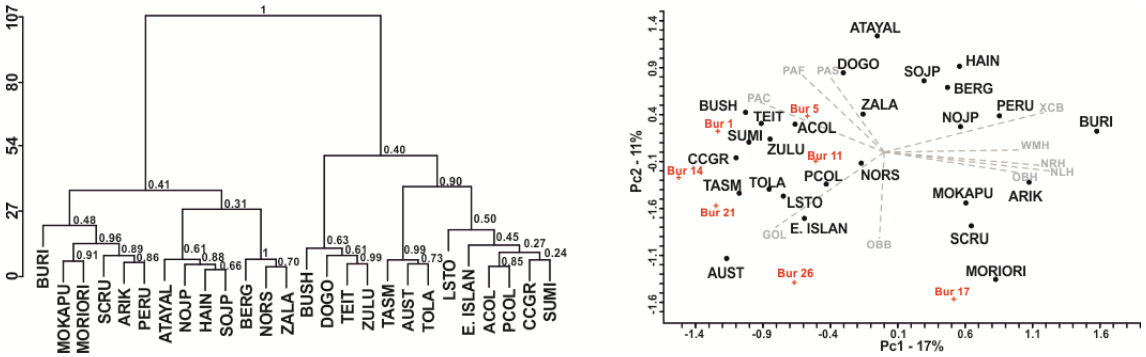

Figure 7. Morphological affintiies of Lapa do Santo crania. Left: Wards cluster based on Mahalanobis distance between craniometric data from worldwide populations and Lapa do Santo (see Supplementary Material for details). The frequencies associated to each branch represent how strong the clusters are, based on 1000 bootstraps of the data. Right: Scatterplot of the series according to the first two Principal Components extracted from the complete dataset. Centroids are plotted in black; Lapa do Santo individuals are plotted in red. The gray lines and labels represent the correlations between the original variables and each of the PCs. Only correlations larger than 0.5 were plotted. Correlations are scaled to the axis dimensions, i.e., perfect correlations (r=1.0 or r=-1.0) would touch the limits of the graph.

Figure 8. Lapa do Santo Mortuary Pattern 1. a, Picture of Burial 1 after the stones that were covering the skeleton were removed. b, Picture of the north-east corner of unit L11 during the initial stages of exhumation of Burial 27. c, Picture of Burial 27 with an open mandible indicating the grave was not fully filled with sediments after inhumation.

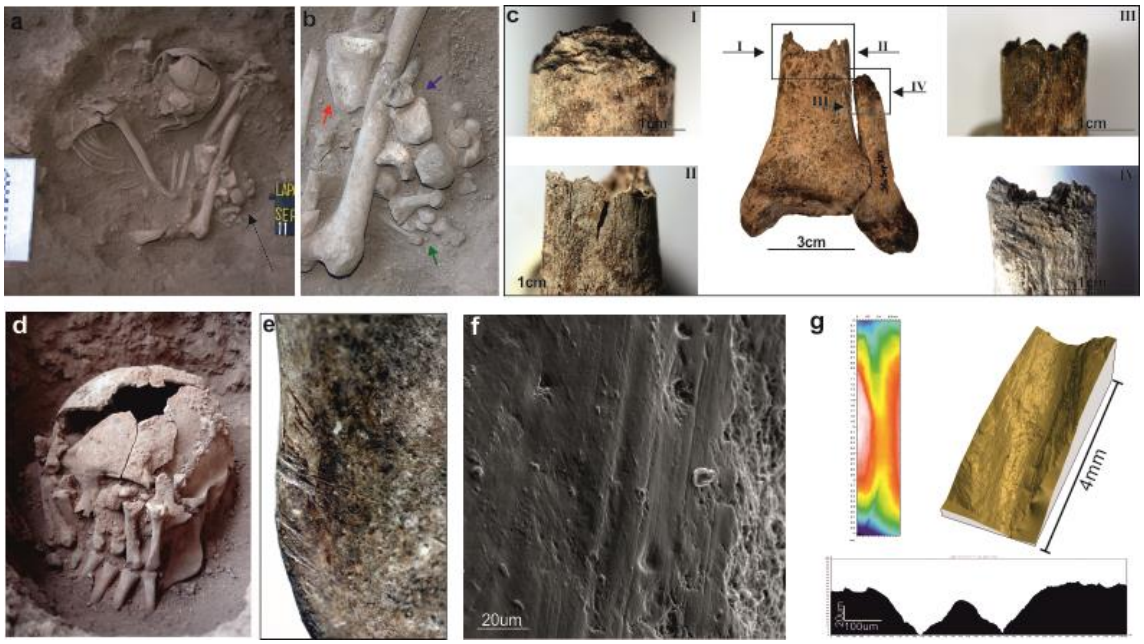

Figure 9. Lapa do Santo Mortuary Pattern 2a: a, Burial 21 from Lapa do Santo after removing stones covering the grave. Note that although fully articulated the midshafts of the lower legs were absent (black arrow). b, Detail of Burial 21's bones that were directly involved in the mutilation processes. The distal extremities of the chopped left tibia and fibula (blue arrow) and the bones of the feet (green arrow) were articulated. The proximal extremity of the right tibia (red arrow), however, was not in connection with the distal extremity of the right femur. c, Distal extremities of the articulated left tibia and fibula. Note that only the portion of the bones that would have been in contact with the skin (I and IV) presents chop marks confirming cutting took place while soft tissues were still present. d, Burial 26. Picture of the decapitated head with the hands resting over the face. e, Burial 26`s right mandibular ramus exemplifying the cut marks found in the bones. f, Scanning electron microscopy of the cut-mark in Burial 26' mandible showing parallel micro-striation. g, Top: Topography and digital 3D model of a cut-mark in Burial's 26 mandible generated using confocal microscopy. The parallel micro-striations can also be observed. Bottom: Cut-mark transection depicts a V-shaped profile.

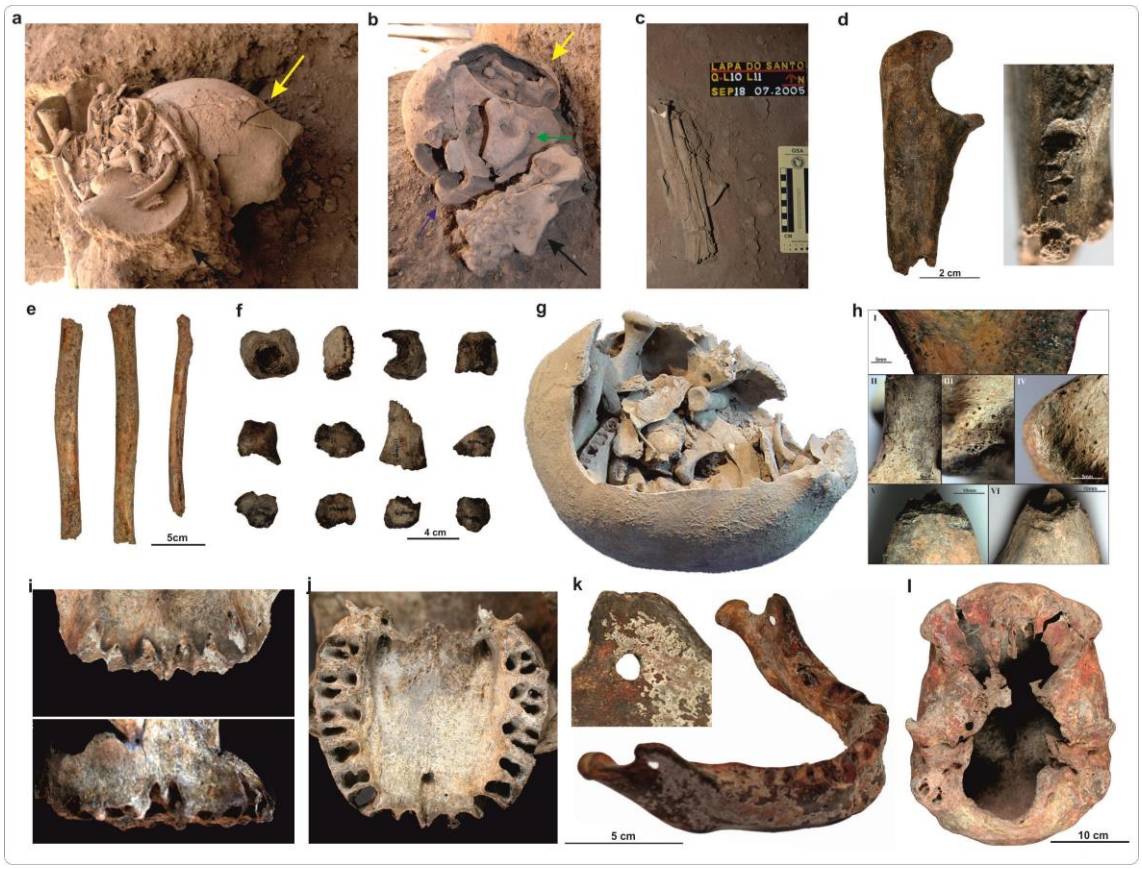

Figure 10. Lapa do Santo Mortuary Pattern 2b: a, Field picture of Burial 14 showing the individualized adult cranium (yellow arrow) next to a bundle of post-cranial bones of two infants (black arrow) b, Field picture of Burial 17 showing the individualized adult cranium (yellow arrow) next to a bundle of post-cranial bones of infants (black arrow). The purple and green arrows indicate the left ulna and humerus that are shown in "d" and "h", respectively. Note that inside the cranium several bones can be observed. c, Field picture of Burial 18 showing a bundle composed of four chopped midshafts from adult long bones (same as in "e") that was deposited within the mandible of an infant (same as in k). d, sectioned distal extremity of left ulna found inside Burial 17's crania. In the detail, chopp marks associated with sectioning processes. e, from left to right sectioned midshafts of the left humerus, the right humerus and the right radio. f, chopped sections of burnt long bones that were deposited inside Burial 17's neurocranium. g, The neurocranium of Burial 17 was used as a funerary receptacle inside which chopped and/or burnt bones of the same individual were deposited. h, Mutilated distal extremity of the left humerus from Burial 17 presenting defleshing marks (I-IV) and chop marks (V- VI). i, Burial 17 maxilla has burn marks concentrated in the anterior portion of the external alveoli margin. j, Burial 17's maxillary dentition was intentionally removed prior to the interment. k, Mandible of Burial 18 had teeth removed and holes drilled in its coronoid processes (see detail). l, Cranium of Burial 14 with red pigment and missing face.

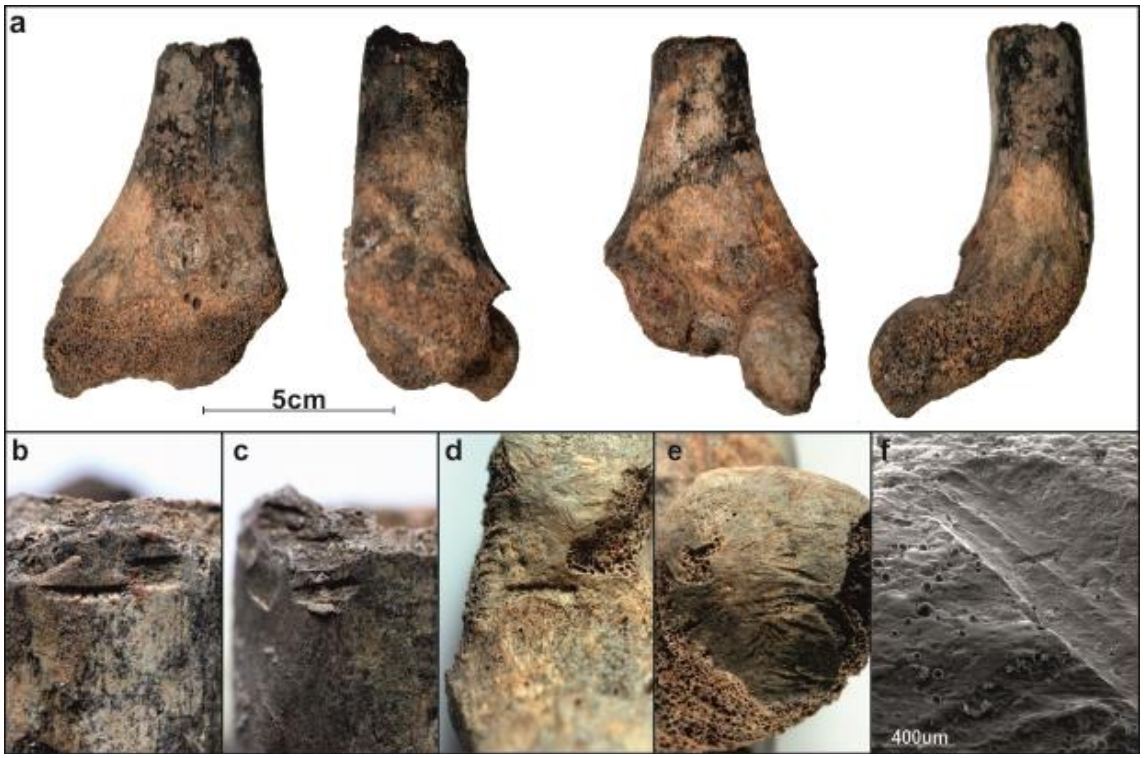

Figure 11. Lapa do Santo Mortuary Pattern 2c. Chopped distal extremity of left femur (LSt-3083) found isolated from other human remains. a, From left to right anterior, lateral, posterior and medial views, respectively. b,c, detail of chopping marks in the anterior and posterior portion of the sectioned margin, respectively. d, incisions present in the posterior region near the articular surface. e, rodent gnawing marks in the articular surface of the medial condyle. f, scanning electron microscopy of the gnawing marks.

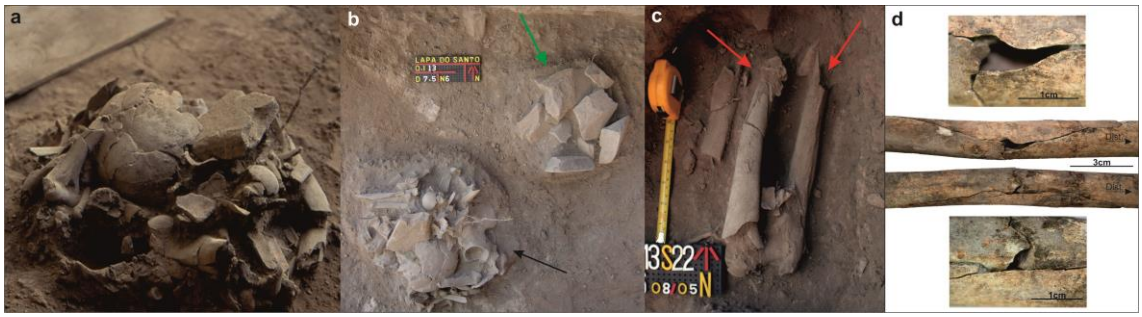

Figure 12. Lapa do Santo Mortuary Pattern 3. a, LSMP-3 was characterized by circular pits completely filled with the non-articulated bones of a single individual. b, Burial 15 (black arrow) is typical of LSMP-3. The picture was taken after the circular structure composed of stones covering the grave was removed. The green arrow points to a circular structure of stones that was not directly associated with any burial. c, Long bones at the bottom of Burial 22's grave exemplify the practice of breaking the midshafts (midshafts). d, Humerus of Burial 22 exemplifying butterfly fracture and impact points (details above and below).